CHALMERS
UNIVERSITY OF TECHNOLOGY

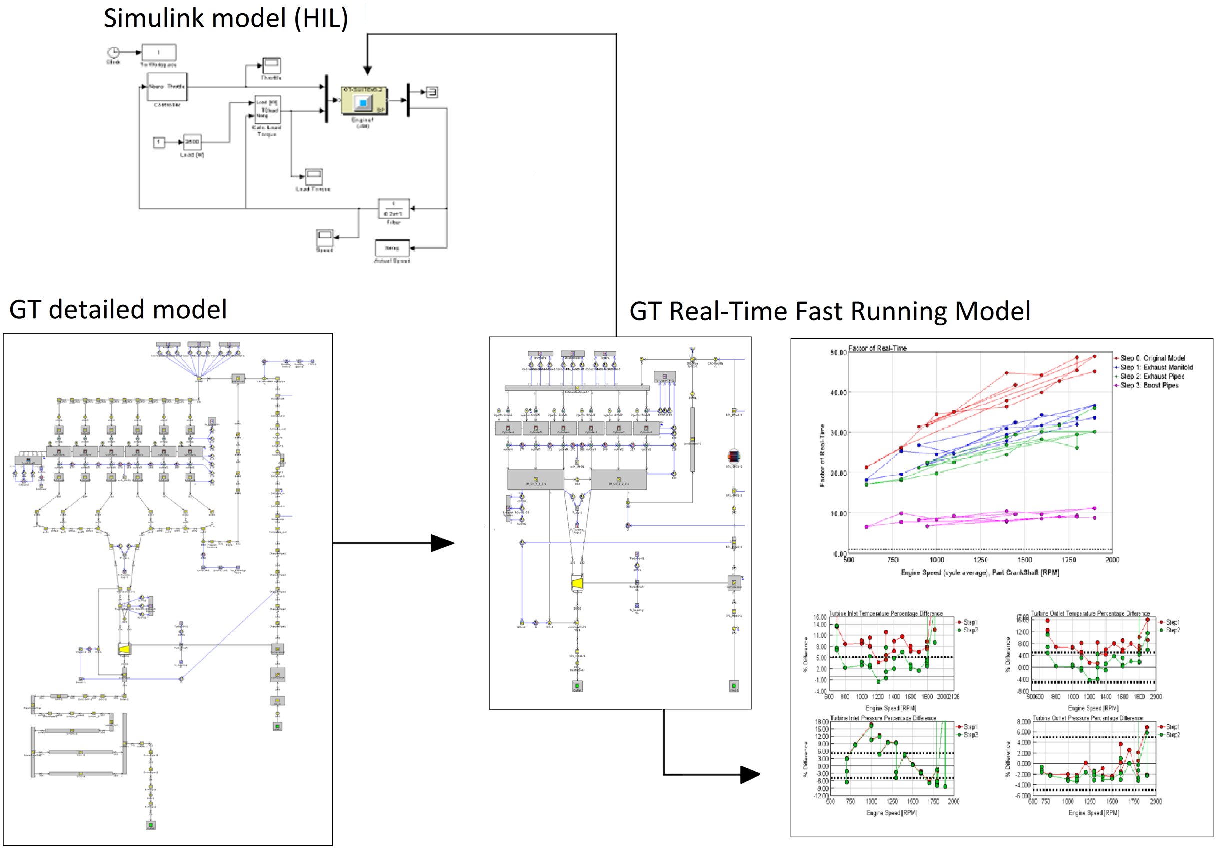
Simulink model (HIL)
GT detailed model
GT Real-Time Fast Running Model
Factor of Real-Time
Step 0: Original Model
Step 1: Exhaust Manifold
Step 2: Exhaust Pipes
Step 3: Boost Pipes
Engine Speed (cycle average), Fast CrankShaft [RPM]
Turbine Inlet Temperature Percentage Difference
Turbine Outlet Temperature Percentage Difference
Turbine Inlet Pressure Percentage Difference
Turbine Outlet Pressure Percentage Difference
% Difference
Engine Speed [RPM]
Step1
Step2

Fast Running 1D model of a heavy-duty diesel engine

Master’s thesis in Automotive Engineering

ADAM ERLANDSSON

Department of Mechanics and Maritime Sciences
CHALMERS UNIVERSITY OF TECHNOLOGY
Gothenburg, Sweden 2017

Master's thesis in Automotive Engineering

Fast Running 1D model of a heavy-duty diesel engine

ADAM ERLANDSSON

Department of Mechanics and Maritime Sciences
Division of Combustion
Chalmers University of Technology
Gothenburg, Sweden 2017

Fast Running 1D model of a heavy-duty diesel engine

ADAM ERLANDSSON

© ADAM ERLANDSSON, 2017.

Industrial supervisor: Dr. Ethan Faghani, Volvo Penta AB
Academic supervisor: Dr. Jelena Andric, Division of Combustion, Department of Mechanics and Maritime Sciences, Chalmers University of Technology
Examiner: Assoc. Prof. Jonas Sjöblom, Division of Combustion, Department of Mechanics and Maritime Sciences, Chalmers University of Technology

Master's Thesis 2017:37
ISSN 1652-8557
Department of Mechanics and Maritime Sciences
Division of Combustion
Chalmers University of Technology
SE-412 96 Göteborg
Sweden
Telephone +46 (0)31 772 1000

Cover: Visualization of the Fast Running Model´s role in the chain of a detailed GT model and the use of a HiL environment.

Chalmers Reproservice
Gothenburg, Sweden 2017

Fast Running 1D model of a heavy-duty diesel engine
Master's thesis in Automotive Engineering
ADAM ERLANDSSON
Department of Mechanics and Maritime Sciences
Chalmers University of Technology

Abstract

This thesis deals with creation of one-dimensional (1D) Fast Running Model (FRM) for a heavy-duty diesel engine for the purpose of Hardware-in-the Loop (HiL) virtual testing. The FRM was created from a detailed model of a Volvo Penta D13 engine. Investigation of the effects of different calibration practices was carried out on the sub-system level. The conversion procedure and the best calibration practices are presented in detail. The obtained FRM reached real-time while running on the HiL VIRtual TEst Cell (VIRTEC) at Volvo Penta, while yielding satisfactory results for engine performance.

Keywords: Engine model, FRM, HiL, virtual testing, calibration, Real-Time, Volvo Penta.

Acknowledgements

First of all, I would like to acknowledge indisputable, most patient and greatest technical help through this master thesis project, directing the biggest thank you towards Daniel Schimmel from Gamma-Technologies, whose input and guidance were something exceptional. Thank you!

Second of all, I would like to thank my official supervisors. Jelena Andric from Chalmers for her continuous reminders, structuring and planning in beforehand. Thank you! Ethan Faghani, my industrial supervisor at Volvo Penta. Always grateful for the opportunity and daily feedback throughout the whole project. Thank you!

On the same note, I also want to express gratitude to Volvo AB for recruiting me, including Mario Celegin, and letting me work on the site for most of the time despite the fact that the spacing was very restricted during the time being. Not to forget all the personal I talked to and got to know better in-between all the work, the welcoming and the kindness. Thank you for my first and very positive experience!

Jonas Sjöblom, Director of the Master Programme Automotive Engineering and my examiner. Despite your precious and limited time, you always showed a great interest and was very excited about the project, it is indeed contagious! Thank you!

Thanks to Keerthivash Chellamalai for his contribution and inputs!

To not forget to mention and acknowledge the support contributed by Fordonsstrategisk Forskning och Innovation (FFI) and Vinnova. This manuscript was written as a part of Virtual Engine Calibration (VirCal) project funded by FFI. The thesis had a sub-part in the whole, where Volvo Penta AB, Gamma Technologies and Chalmers had a joint project. Very exciting project and always grateful for my participation and I wish to thank all participators making it possible.

The very last but not least, I want to thank my family and friends for their understanding and support during this master thesis project. Thank you!

Adam Erlandsson, Gothenburg, June 2017.

Contents

List of Figures **xiii**

1 Introduction **1**
- 1.1 Aim 2
- 1.2 Objective 3
- 1.3 Borders and limitations 3

2 Theoretical and Modelling Background **5**
- 2.1 Governing Equations 5
- 2.2 Discretization 6
  - 2.2.1 Explicit Method 7
  - 2.2.2 Timestep 8
- 2.3 Combustion Model 9
- 2.4 GT-POWER 9

3 Engine Modelling **11**
- 3.1 Detailed Engine Model 11
- 3.2 Fast Running Model 13
  - 3.2.1 Engine Operating Range 13
- 3.3 General FRM conversion 15
  - 3.3.1 **T**agging 15
  - 3.3.2 **V**olume simplification 16
  - 3.3.3 **C**alibration 18
    - 3.3.3.1 **M**inimizing approach 18
    - 3.3.3.2 **T**arget approach 18
  - 3.3.4 **V**alidation 18
- 3.4 Factor of Real-Time 21
- 3.5 Detailed Conversion Procedure 22
  - 3.5.1 Exhaust Manifold 22
    - 3.5.1.1 Volume Reduction 22
    - 3.5.1.2 Calibration 23
  - 3.5.2 Exhaust Pipes 24
    - 3.5.2.1 Volume Reduction 24
    - 3.5.2.2 Calibration 24
  - 3.5.3 EGR Pipes 25
    - 3.5.3.1 Volume Reduction 25

3.5.3.2 Calibration 25
3.5.4 Boost Pipes 25
3.5.4.1 Volume Reduction 25
3.5.4.2 Calibration 27
3.5.5 Intake Manifold 27
3.5.5.1 Volume Reduction 27
3.5.5.2 Calibration 27
3.5.6 Intake Pipes 28
3.5.6.1 Volume Reduction 28
3.5.6.2 Calibration 28

4 Results and Discussion 29
4.1 The Final FRM Model 29
4.1.1 Factor of Real-Time 29
4.1.2 Timestep Angle 30
4.1.3 Compressor and Turbine Temperatures 31
4.1.4 Compressor and Turbine Pressures 32
4.1.5 Airflow Rate 32
4.2 Best calibration practice 33
4.2.1 Intake Pipes 34
4.2.2 Boost Pipes 36
4.2.3 Exhaust Manifold 37
4.2.4 Exhaust Pipes 38
4.2.5 Comments 39

5 Conclusions and Future Work 41

Bibliography 43

A Appendix I
A.1 Governing Equations Derivation I
A.1.1 Reynolds Transport Theorem II
A.1.2 Mass conservation III
A.1.3 The Linear Momentum Equation IV
A.1.4 The Energy Equation V
A.2 Emission Result VI
A.2.1 NO_x, Nitrogen Oxides VI
A.2.2 HC, Hydrocarbons VIII
A.2.3 CO_2, Carbon-dioxides X
A.3 FRM General Modelling Blue Print X
A.3.1 Intake Environment XI
A.3.2 Intake Pipes XI
A.3.3 Compressor XII
A.3.4 Charge Air Cooler (CAC) XIII
A.3.5 CAC-throttle XIV
A.3.6 Intake Manifold XIV
A.3.7 Intake Valves XV

A.3.8 Injectors XV
A.3.9 Cylinder XVI
  A.3.9.1 DI-Pulse XVI
    A.3.9.1.1 Cylinder Pressure Matching XVII
    A.3.9.1.2 Calibration XVIII
A.3.10 Exhaust Valves XIX
A.3.11 Crankshaft with auxiliary XIX
A.3.12 Exhaust Manifold XX
A.3.13 EGR Pipes XXI
A.3.14 Turbine XXII
A.3.15 Wastegate XXII
A.3.16 Turbo Shaft XXIII
A.3.17 Exhaust Pipes XXIV

List of Figures

2.1 Spatial discretization of a pipe. 7

3.1 Detailed model - Defined sub-systems for the D13 engine model . . . 12
3.2 Normalized injected fuel mass over a steady-state speed load sweep. . 14
3.3 27 normalized data points for representation of the engine´s total operating area. 14
3.4 Exemplification of a tagged sub-system, the intake manifold. 16
3.5 Conversion of detailed intake manifold to a FRM with illustration of the reduced number of volumes. 17
3.6 The change in Factor of Real-Time for each system reduced, one after the other. 20
3.7 Turbine properties - Temperatures and pressure percent difference, inlet and outlet. 20
3.8 The reduction step of volumes for the exhaust manifold sub-system. . 23
3.9 The reduction step of volumes for the exhaust pipes´ sub-system. . . 24
3.10 The reduction step of volumes for the EGR pipes´ sub-system. 25
3.11 The reduction step of volumes for the boost pipes´ sub-system. . . . 26
3.12 The reduction step of volumes for the intake manifold sub-system. . . 27
3.13 The reduction step of volumes for the intake pipes´ sub-system. . . . 28

4.1 The final Factor of Real-Time accomplished for the FRM model . . . 29
4.2 The resulting time step in CAD for both detailed model and FRM. . 30
4.3 The percent difference for compressor and turbine temperatures, inlets and outlets. 31
4.4 The percent difference for compressor and turbine pressures, inlets and outlets. 32
4.5 The resulting percent difference for the airflow rate. 33
4.6 Calibration results for airflow rate using two calibration points maximum airflow and maximum engine speed. 34
4.7 Calibration result for compressor inlet pressure using two calibration points: maximum airflow and maximum engine speed. 35
4.8 Boost Pipes - Pressure and massflow minimization approach, using max engine speed and max airflow as calibration points. 36
4.9 Exhaust Manifold - Minimizing pressure and temperature difference, using max engine speed and airflow as calibration points. 37
4.10 Exhaust Pipes - Airflow rate and turbine outlet pressure percentage difference, using maximum airflow point for calibration. 38

4.11 Exhaust Pipes - Turbine inlet and outlet temperature percentage difference, using maximum airflow point for calibration. 38

A.1 Control volume enclosing a fluid flow. II
A.2 NO_x percentage difference, simulated versus measurements. VI
A.3 NO_x ppm absolute difference, simulated versus measurements. VII
A.4 Normalized NO_x ppm values, simulated versus measurements. VII
A.5 HC error percentage, simulated versus measurements. VIII
A.6 HC ppm absolute difference, simulated versus measurements. IX
A.7 Normalized HC ppm data, simulated versus measurements. IX
A.8 CO_2 mole fraction absolute values, simulated versus measurements. . X
A.9 Intake Environment XI
A.10 Intake Pipes XI
A.11 Compressor object XII
A.12 CAC object XIII
A.13 CAC-throttle XIV
A.14 Intake manifold XIV
A.15 Valve object XV
A.16 Injector object XV
A.17 Cylinder object XVI
A.18 Exhaust valve XIX
A.19 Crankshaft and auxiliary XIX
A.20 Exhaust manifold XX
A.21 EGR valve XXI
A.22 Turbine object XXII
A.23 Wastegate object XXII
A.24 Turbo shaft object XXIII
A.25 Exhaust pipes XXIV

1

Introduction

The automotive industry has grown by huge leaps in the recent decade, especially automotive powertrains have seen significant improvements in performance driven by consumer demand and emission regulations. The internal combustion engine is an integral part of modern automotive powertrains used worldwide as an energy converter, transforming chemical energy into mechanical work. The relative low cost of the utilization of an ICE makes it most attractive in multiple applications, e.g. in marine, industry, truck or car sector to mention a few areas. The trend in automotive industry moves towards electrification and a greener approach as natural resources and legislation become more exploited and sophisticated respectively. Nevertheless, the technology of electric motors and batteries has its limitations which speaks for the argument that the ICE will be used in foreseeable future(8). Moreover, the potentials of internal combustion engines can be improved by implementation of advanced technologies.

The implementation of these technologies requires complex control system which ensure adequate engine performance under different operating condition while also regulating engine output emissions. The engine management systems employ microprocessors in conjunction with electronic sensors and actuators in modern engines. This has become very practical in modern heavy duty diesel engines which use high pressure common rail injectors that require precise control of the injection pressure and consequently the injection timing which affect the performance and emission characteristics(2).

The development of such controls unit is a tedious, time consuming and labour intensive. The testing of control logic and calibration of hardware contribute heavily to the difficulty of developing a complex control unit which has to regulate multiple engine subsystems. Testing and verification of the Engine Management System (EMS) is of a great importance and it is hence essential to reduce the development time as well as the costs involved. As a result, there is an inherent need for development methods which are efficient, reliable and accurate while also catering to reduced time and cost(1).

In this context, modeling based approach is beneficial and desirable in the development of modern powertrains. Hardware-in-the-Loop (HiL) technology has become an indispensable tool for development and verification of engine control and management from research to production phase. as Hardware-in-the-Loop (HiL)(4). The HiL is a virtual test-rig with the physical ECU, some physical actuators, and an engine model. With present hardware and computational, HiL simulation environments require simulation models that are able to run in real time or faster. Therefore, one of the main challenges that automotive companies face is to create fast running models that are sufficiently accurate for predicting the underlying physics of phenomena of interest(2).

When developing real-time capable engine models, one needs to consider both the application and and the model predictive capabilities. The mean value modelling approach is characterized by computational speed faster than Real-Time (RT). However, this approach does not predict engine breathing and combustion, and hence it is not advisable anymore. A more suitable approach is to use a 1D Fast Running Model (FRM) that captures gas dynamics and predicts cylinder combustion in crank-angle resolution(6).

FRMs are typically created from the corresponding detailed engine model. The detailed geometry is simplified into coarse one and the gas dynamics remains captured. In this manner the number of computations per time step is reduced, making it possible for the model to run in real time or faster. Importantly, the cylinder combustion remains resolved in crank-angle resolution just as in the detailed model. Employing predictive, crank-angle-degree resolved combustion models that can be re-calibrated is essential for HiL simulations(4)(3).

The thesis work deals with the conversion of the detailed GT-POWER model of a D13 Volvo Penta engine into the FRM to be ultimately used in the VIRTEC (VIRtual Test Cell) HiL system. The present work is a part of the joint VirCal (VIRtual CALibration) project between Chalmers and Volvo Penta.

This Master thesis was performed as a part of the joint project between Volvo Penta and Chalmers University of Technology.

1.1 Aim

This project aims at developing predictable real-time capable engine model that is suitable for virtual testing. It includes the following main steps:

- Development of a real-time capable model based on the engine configuration and measurement data but without a detailed model.
- Increasing the model flexibility and reducing the efforts needed for model calibration.
- Increased knowledge in component modelling in general.

- Ensuring high model fidelity to accurately predict engine performance and exhaust emissions.

1.2 Objective

- Conversion of the detailed GT-POWER model of the Volvo Penta D13 engine into the FRM.
- Detailed description of the conversion process for all relevant subsystems.
- Calibration of the FRM including the description of the important calibration parameters and operating points.
- Verification of the calibrated FRM.
- Description of best practices for component calibration.

1.3 Borders and limitations

- The models will not be improved to even greater accuracy than the baseline detailed model.
- Computational speed is of a greater interest rather than accuracy. The accuracy is of importance, hence it should be good enough. Thus, within given tolerances or close-by.
- Aftertreatment won´t be a field of topic more than analyzing emissions data.
- Further investigation in combustion and heat transfer models is outside the objective.
- No further interest in test cells rather than using test cell data is an input and for calibration. In the end, the measurements will be compared with simulated data. The test cell data is a steady-state speed sweep.
- Engine design is not within the scope as the model created should represent the same engine.
- Testing the model in a HiL-system is out of the range and is externally taken care of.
- NN is not performed internally, nonetheless will be a practice used to support the thesis if needed.
- If used, Simulink will be used for process data only, the responsibility is within the integration between GT-POWER and Simulink.
- The FRM is derived from an existing engine, thus not a FRM from scratch.
- It will not be verified with a driving cycle of any sort due to time constraint.

2

Theoretical and Modelling Background

In the following sections the underlying theory will be explained and presented. It will focus on the essential material regarding FRMs. Discretization, solver, run speed, governing equations and heat transfer will be the subjects of matter for deeper understanding.

2.1 Governing Equations

This section will present the governing equations used in the commercial 1D modeling software GT-POWER, describing the laws of nature considering fluid dynamics.

The laws of mechanics are written for one defined system, one fixed mass. These laws specify what happens when the defined system interact with its surroundings, where the boundaries separates the externalities and the system. The system approach let us establish a dynamic mechanical analysis of the environment. With that spirit in mind, fluids in motion (fluid dynamics) can also be studied by converting a system analysis to a control volume analysis. In fluid dynamics, specific regions are the subject of matter rather than individual masses and the system particles only occupy the laws for only an instant, until the next system of particles arrive. There is a need of converting the basic mechanical system laws to a control volume approach. Reynolds Transport Theorem (RTT) can be applied to all the basics mechanical laws and re-write them into control volume form. By doing so, the result is the Navier-Stokes equations. Namely, comprising the mass conservation equation, the momentum equation and the energy equation. The expressions presented are simplified for unsteady compressible one-dimensional fluid flow, since those fairly represent the flow within an engine. The full derivation can be found in appendix whilst the end result from the derivation will be presented without further ado(7).

Mass Conservation

$$\int_{cv} \frac{\partial \rho}{\partial t} dV + \sum_{m} \left(\rho_m A_m \mathbf{V_m}\right)_{out} - \sum_{n} \left(\rho_n A_n \mathbf{V_n}\right)_{in} = 0 \tag{2.1}$$

The first term in equation 2.1, $\int_{cv} \frac{\partial \rho}{\partial t} dV$, is the change within the control volume (CV) with ρ as the density which is not constant. Note that CV and CS stand for "control volume" and "control surface", respectively. Evidently, dA and dV stands for an infinite small control surface and control volume respectively. The other terms describe the flow in and out over the control surface and are often referred to as the flux terms. Considering the flux terms, the sign convention depends on the direction of the normal unit vector ($\mathbf{n}$). The velocities V_n and V_m are the cosine or normal component of the relative velocity between the fluid and the control volume, and A is the control surface area. The indices "m" and "n" stands for the vector and scalar properties belonging to the out- and in-going fluid(7).

The Momentum Equation

$$\sum \mathbf{F} = \int_{cv} \frac{\partial}{\partial t} \rho \mathbf{V} dV + \sum_{m} \left(\dot{\mathbf{m}}_{\mathbf{m}} \mathbf{V}_{\mathbf{m}} \right)_{out} - \sum_{n} \left(\dot{\mathbf{m}}_{\mathbf{n}} \mathbf{V}_{\mathbf{n}} \right)_{in} \tag{2.2}$$

The force $\mathbf{F} = \left[F_x, F_y, F_z \right]$ is determined from the net result of the right hand side of the impetus equation above. $\dot{\mathbf{m}}$ is the massflow through the control areas(7).

The Energy Equation

$$\dot{Q} - \dot{W}_s - \dot{W}_v = \frac{\partial}{\partial t} \Big[\int_{cv} \left(\hat{h} + \frac{1}{2} \mathbf{V}^2 + \mathbf{g} z \right) \rho dV \Big] + \int_{cs} \left(\hat{h} + \frac{1}{2} \mathbf{V}^2 + \mathbf{g} z \right) \rho V_n dA \tag{2.3}$$

$$\int_{cs} \left(\hat{h} + \frac{1}{2} \mathbf{V}^2 + \mathbf{g} z \right) \rho V_n dA = \sum \left(\hat{h} + \frac{1}{2} \mathbf{V}^2 + \mathbf{g} z \right)_{out} \dot{m}_{out} - \sum \left(\hat{h} + \frac{1}{2} \mathbf{V}^2 + \mathbf{g} z \right)_{in} \dot{m}_{in} \tag{2.4}$$

Starting with equation 2.3 above, $\dot{Q}$ is the heat added to the system. $\dot{W}_s$ is the work performed from the system and $\dot{W}_v$ is the shear work due to viscous stresses of the control surface. The negative convention implies work performed on the surroundings. The term in the parentheses "$\left(\hat{h} + \frac{1}{2} \mathbf{V}^2 + \mathbf{g} z \right)$" represent the sum of different energies. $\hat{h}$ is the internal energy, $\frac{1}{2} \mathbf{V}^2$ is the kinetic energy and $\mathbf{g} z$ is the potential energy. $\mathbf{g}$ is the gravitational constant and z is the vertical distance from any arbitrary coordinate system defined. Equation 2.4 is the expanded flux term.

2.2 Discretization

Two different discretizations are present, i.e. both in space and in time. Both space and time discretization are discussed in this subsection(5).

The piping system itself is a discrete system of volumes (spatial grid), continuously it can be further divided into sub-volumes. For example, one pipe (one volume) can be discretized into several sub-volumes, which contain events of computations at every time step. Figure 2.1 illustrates the spatial discretization of a pipe(5).

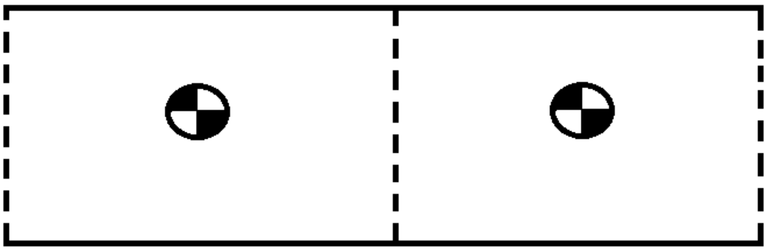

Figure 2.1: Spatial discretization of a pipe.

A coarser discretization leads to shorter simulation run time. Although, the gain is simulation speed, the compromise would be the accuracy. On the contrary, finer resolution normally result in the sacrifice of simulation run time with having reliable accuracy instead. However, there is a limit whereas refining the resolution is of no advantage, i.e. the refined discretization only add up computational time without improving the accuracy. The objective could be to find this limit, where maximum accuracy is achieved using the greatest discretization length possible. Depending on the solver used, the discretization length has different impacts. Although, for both the implicit and the explicit solver, with refined discretization the computational time will grow. The reason is the creation of more sub-volumes this imply, where calculations are performed regarding the fluid flow. From hereon, the Courant criteria will be the difference. The explicit method has a proportional dependency between sub-volume discretization and timestep size, due to the usage of the Courant criterion. Smaller discretization requires smaller timesteps for the solution to be numerically stable and thus more computationally heavy. Moreover, the explicit solver will henceforth be discussed to explain how quantities are calculated using the spatial and time discretization grid(5).

2.2.1 Explicit Method

The solved quantities are averages across the flow pathway and thus defined as one-dimensional (1D) flow. The partial differential equations can be integrated over time using either implicit or explicit method. As previously mentioned, the natural continuous geometry is discretized into sub-volumes in order to enable numerical calculations. Every pipe is sectioned into at least one sub-volume and all flowsplits are single volumes at all times. Boundaries connect the adjacent sub-volumes where vector variables are calculated. Scalar quantities are calculated at the centers of the sub-volumes, as seen in figure 2.1. Massflow rate, internal energy and density are the primary solution variables used for the explicit method and are input for the conservation equations. The explicit method calculates the state of the system at the next time step from the state at the current timestep. Thus, the right hand side of the Navier-Stokes equations is known by implementing values from the current timestep. The derivative is known and the partial differential equations are integrated over the timestep, thereby utilizing the adjacent volumes and the boundary conditions. Specifically, in every sub-volume border, the NS momentum equation is computed. This setup is referred to as staggered grid when vector quantities are calculated on the borders and scalar values in the centre. This solver tends to be stiff, meaning too large timesteps will create amplified errors of exponential growth, hence small timesteps are required. The timestep size is restricted by the Courant condition and will ensure numerical stability, which will be discussed henceforth. The small timesteps required for this solver option makes it undesirable for relative longer simulation runs. However, the explicit solver is desirable whenever high resolution is needed to capture the flow behaviour, e.g. to capture highly unsteady flow. Nonetheless, if accurate pressure pulsations and wave dynamics are of a greater priority, the explicit method is recommended. Temperature and pressure for each timestep are calculated in the following ways(5):

I] The mass and energy in one volume are obtained through the energy and continuity equations.
II] As the mass and the volume are known variables, the density is computed and resulting in two more known, the density and energy.
III] All the mentioned equations of state for each kind determine energy and density as a function of temperature and pressure. The solver will run a pre-set of patches with values on temperature and pressure until they satisfy the previously calculated species, i.e. density and energy(5).

The timestep will be discussed to complete the information about the solver.

2.2.2 Timestep

The explicit method is a non-iterative method, depending on the current and neighbouring volumes´ states. Therefore, when calculating quantities such as temperature and pressure it needs criteria for numerical stability. Hereby, the Courant condition is introduced, which restricts the timestep. Basically, next calculation cannot be performed to far from the current one, since it is a neighbouring dependency between them. An infinite small step from the current volume should return a small change in the calculated quantities for the next one coming. This will ensure a more refined discretization and more accurate results by default. Moreover, the Courant criteria relates the timestep and the discretization length. The sub-volume length is nothing less than the discretization length of a pipe. In practice, the solver choose its timesteps to meet the following Courant condition(5):

$$\frac{\Delta t}{\Delta x}\Big(|u| + c\Big) \leqslant 0.8 * m \tag{2.5}$$

$\mathbf{\Delta t}$ is the timestep, $\mathbf{\Delta x}$ is the discretization length, **u** is the local flow velocity, **c** is the speed of sound, m is the timestep multiplier and 0.8 is derived from actual fluid physics.

2.3 Combustion Model

The general calculations will be described in this section. The engine model utilizes a fully predictive combustion model(4). The usage of a fully predictive combustion model takes into account in-cylinder variations during the combustion. It takes more parameters into account while calculating a unique burn rate for every other engine operating point. This means that, depending on the engine operating point conditions with different load, rpm, EGR, residuals and e.g. different injection timings, the burn rate is derived. This is referred to a reverse run by the fact that the burn rate is the result from cylinder pressure traces. The predictive combustion model is calibrated against these pressures traces together with very detailed injector data. With further calibration of typical diesel combustion properties, the error between measured cylinder pressure and simulated can come down to a maximum of 1[MPa] difference. Moreover, very detailed information can be found in the appendix section A.3.9.1.

2.4 GT-POWER

GT-POWER is an engine simulation software and is a part of the bigger GT-SUITE package from Gamma Technologies (GT). GT-SUITE can be used to model almost any technical system, stretching from 0D all the way to 3D flow.

The models in the software are highly physical and aiming to mimic the engine technologies such as air filter, compressor, inter-cooler, cylinders and turbine to achieve good accuracy. The model setup can vary to a great extent as different engines are based on different technologies. Most commonly engine models consider cylinders, crankshaft, ports, valves and the piping system. The engine components are connected through the piping system, where different pipes can be represented to establish the flow properly. Everything used in the model of the physical engine is referred to as objects. There is a folder for each component property to capture, depending on what technology is modelled. For example, typical flow objects (pipes) contain geometry, thermal and pressure drop folders. This ensures the object performs as the actual component regarding friction (pressure drop) and heat transfer attributes. However, the inputs to a certain object can be off different nature. It can be a constant value, a parameter, another reference in the constellation of a map or actuators of different sorts. It often depends on the user's resources or scope how much data are used and imposed in the model. Own made calculation circuits can be performed within the model if the default selection is insufficient. The software can predict steady-state or transient engine operation and the outputs could be time resolved, crank-angle or single value quantities.

3

Engine Modelling

First, this section describes the 1D detailed engine model which is used as a baseline model for derivation of a 1D Fast Running Model (FRM). Subsequently, the revision of the FRM is discussed in detail. Lastly, the individual subsystem conversions are presented.

3.1 Detailed Engine Model

The detailed model features of the Volvo D13-700 heavy-duty diesel engine. This is a 6 cylinder 12.8 L displacement engine with a twin scroll variable geometry turbocharger. Figure 3.1 represents the engine model with its subsystems: intake pipes, boost pipes, Charge Air Cooler (CAC), EGR, intake manifolds, cylinders, turbine, and exhaust pipes.

As described in the previous section, the Navier-Stokes equations are solved for each discretised volume in the flow direction. The combustion is modeled using DI Pulse model for diesel engines developed by Gamma Technologies (GT). It is important to note that this is a predictive combustion model, i.e. the burn rate is calculated based on in-cylinder properties. Another important feature of the predictive model is that it can be re-calibrated.

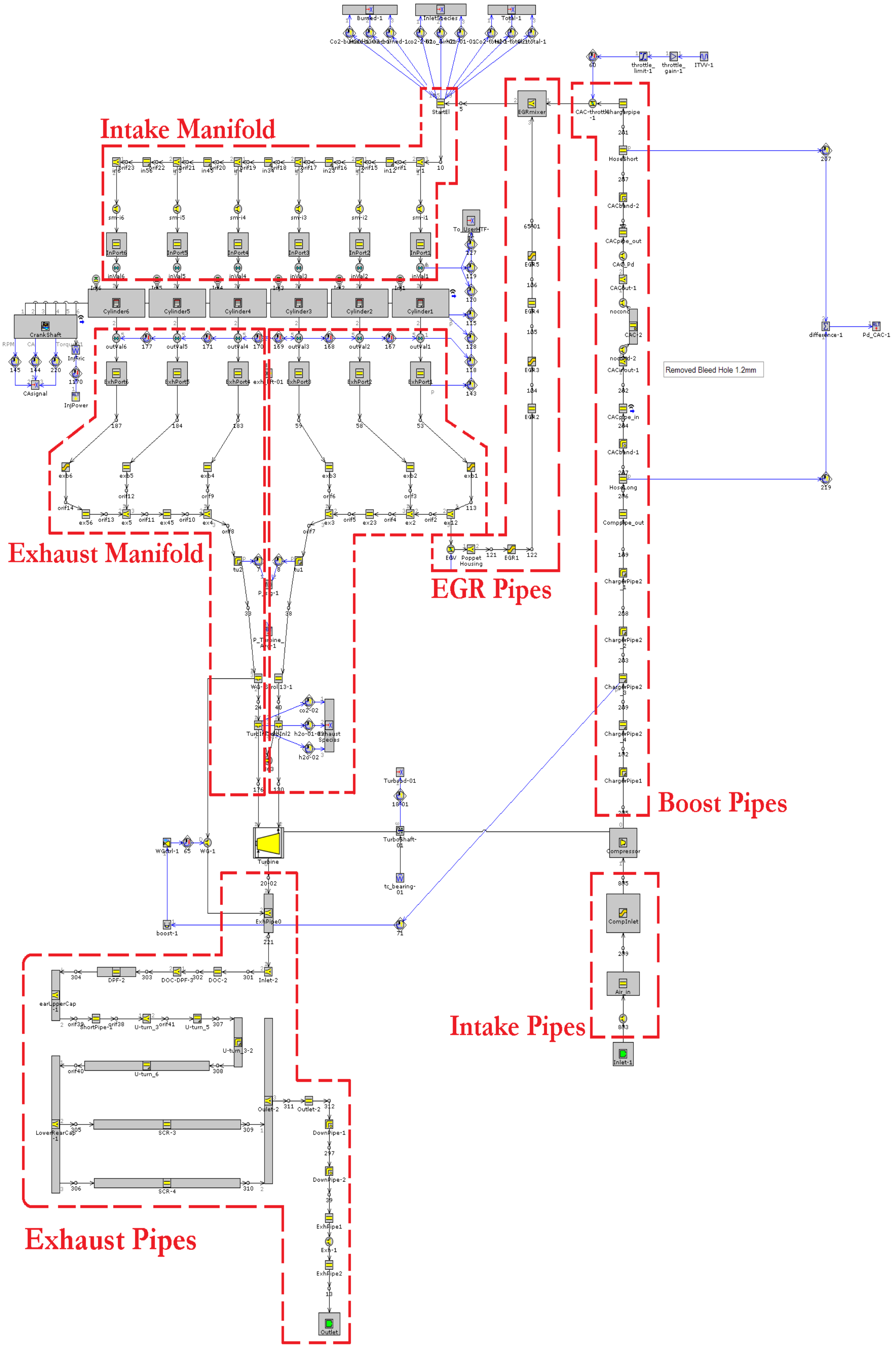
Intake Manifold
Exhaust Manifold
EGR Pipes
Boost Pipes
Intake Pipes
Exhaust Pipes
Removed Bleed Hole 1.2mm
CrankShaft
Cylinder6
Cylinder5
Cylinder4
Cylinder3
Cylinder2
Cylinder1
EGRmixer
Turbine
Compressor
CompInlet
Air_in
Inlet-1
DPF-2
DOC-DPF-3
DOC-2
SCR-3
SCR-4
Outlet
difference-1
Pd_CAC-1

Figure 3.1: Detailed model - Defined sub-systems for the D13 engine model

3.2 Fast Running Model

The detailed model need to be reviewed prior to its conversion to FRM. The following steps need to be undertaken:

- Removal of exhaust manifold heat calculation.
- Removal of intake manifold cylinder wall reference objects, wall temperature and heat transfer calculations.
- Imposition of new cylinder wall reference temperature object for intake manifold from the detailed model for all engine operating points.
- Extraction of burn rates from detail model simulation and imposition onto the model to be converted.
- Extraction of fuel fraction burned from detail model simulation and imposition onto the model to be converted.
- Extraction of start of combustion timing in crank angle degrees from detailed simulation and imposition onto model to be converted.
- Extraction of intake and exhaust valve face and valve back temperature to be included through reference objects.
- Extraction of the cylinder head, piston head and skirt temperatures and subsequently imposition of zone based temperatures.

3.2.1 Engine Operating Range

Experimental data chosen for the FRM calibration and verification correspond to Part Load Map (PLM). The test cell measurements were performed for 169 operating points through a steady-state speed sweep. This means that a specific amount of fuel is injected through the engine´s whole RPM range. Then, the injected mass is lowered and the speed sweep starts once again. This procedure is illustrated in figure 3.2. The speed sweep procedure is replicated until the lowest load is ran through. Steady-state implies that before transition from one engine operating point to the other, the measured values should be fairly stable. The term "Case" used through the report refer to different engine operating points. The numbering of the operating points is from high load to low load, while the engine speed is varying from high to low as well. All operating points from circa case 100 and forth represent low load. Note that higher loads have greater importance since they represent the typical operating area for the engine. Figures 3.2 and are normalized due to the projects confidentiality.

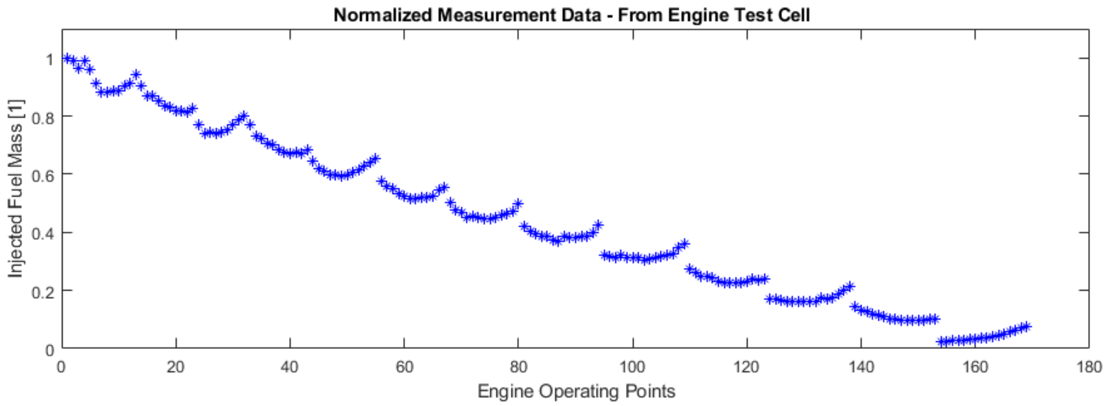

Figure 3.2: Normalized injected fuel mass over a steady-state speed load sweep.

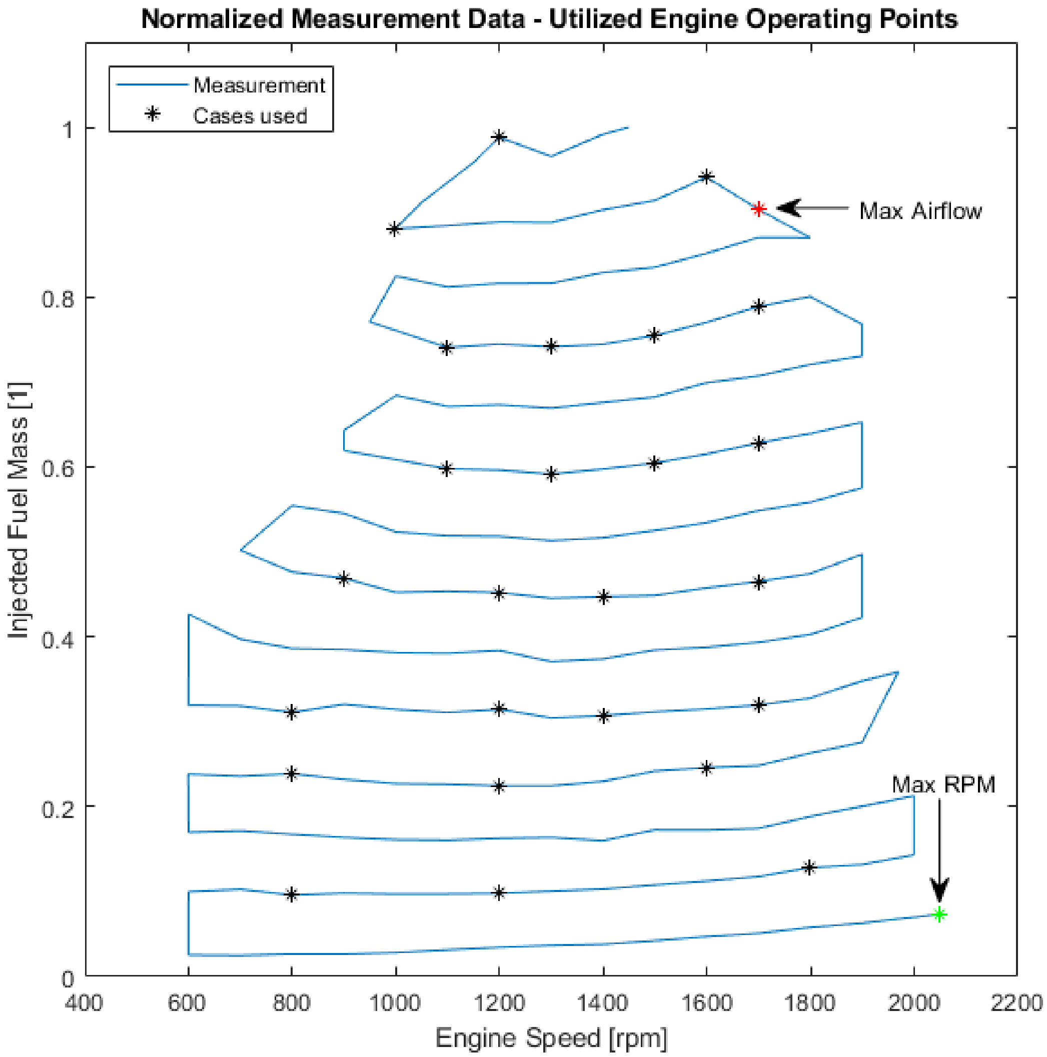

Figure 3.3: 27 normalized data points for representation of the engine´s total operating area.

Figure 3.3 above illustrates 27 points that were chosen to represent the engine operating range. The idea was to represent the mid- and high-load range with more points since those were of greater interest. Noticeably, there are still around ten low load cases represented, counting from vertical axis values of 0.4 and below. It should be noted that, the speed of operation of this diesel powered heavy-duty engine ranges from 600 to 2100 [RPM] with a maximum torque of 2500[Nm] and a power of 700[hp].

3.3 General FRM conversion

The FRM conversion involves the following steps: 3.3.1-3.3.4, to ensure successful volume reduction and yet maintained accuracy.

3.3.1 Tagging

All engine components and subsystems considered for simplifications and calibration need to be tagged. The following subsystems are regarded herein: Intake pipes, boost pipes, intake manifold, exhaust manifold, EGR pipes and exhaust pipes. An example of subsystem tagging is illustrated in figure 3.4 for the sub-system "Intake Manifold".

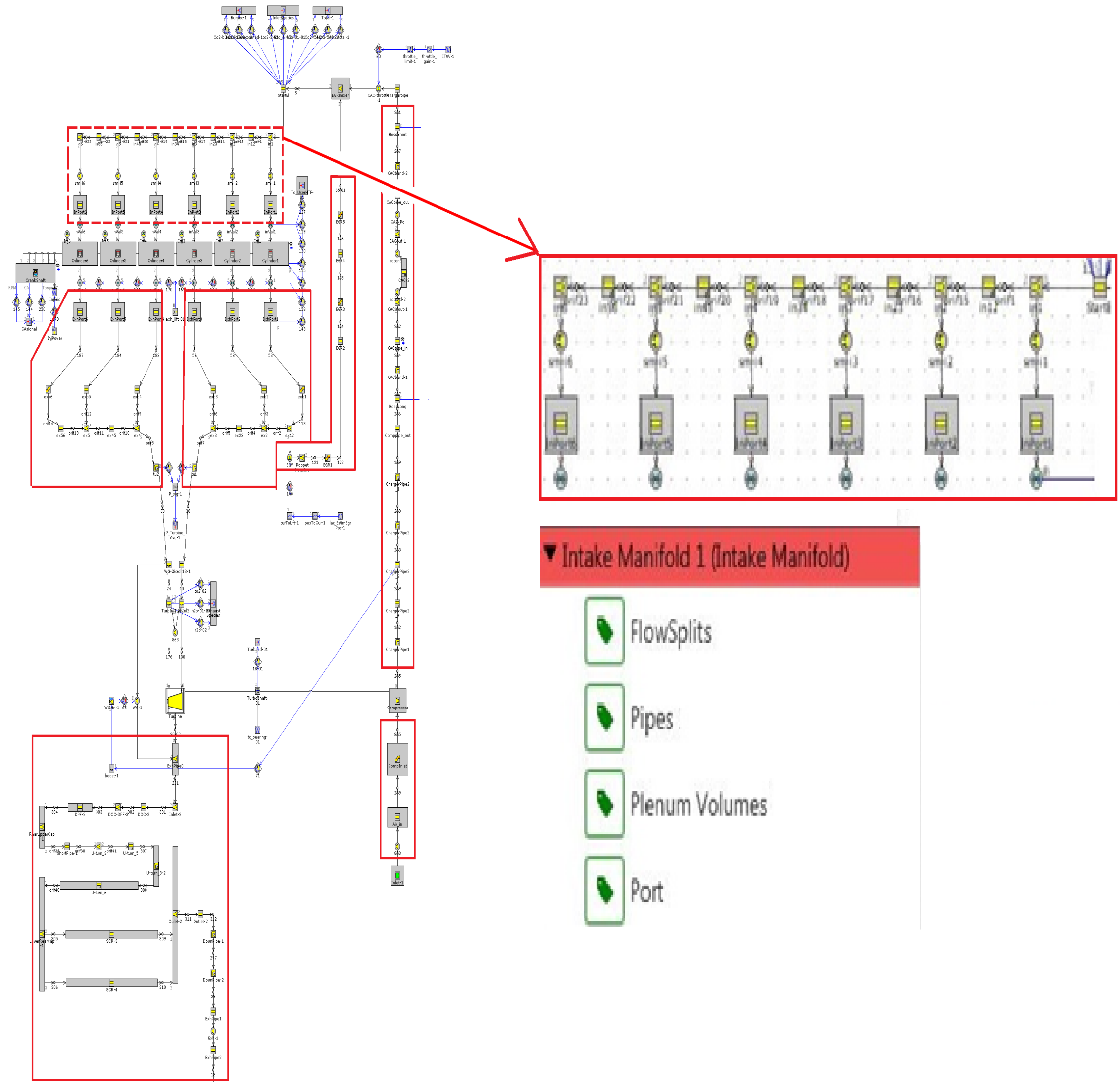
Intake Manifold 1 (Intake Manifold)
FlowSplits
Pipes
Plenum Volumes
Port

Figure 3.4: Exemplification of a tagged sub-system, the intake manifold.

3.3.2 Volume simplification

To simplify the model geometry and hence increase its run speed the flow volumes within a subsystem are lumped into a single pipe or a flowsplit.

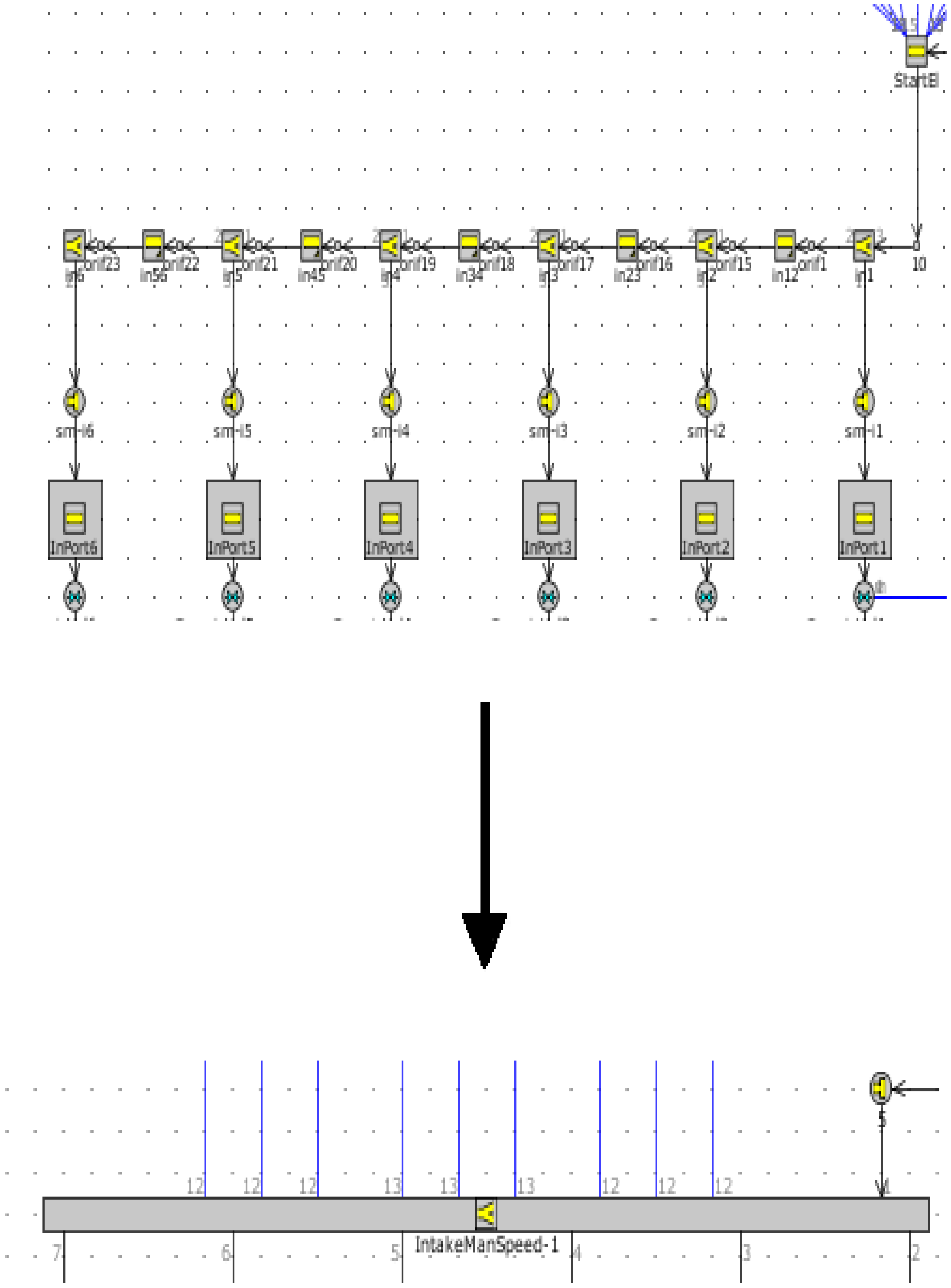
StartBl
10
In6
orif23
In56
orif22
In5
orif21
In45
orif20
In4
orif19
In34
orif18
In3
orif17
In23
orif16
In2
orif15
In12
orif1
In1
sm-I6
sm-I5
sm-I4
sm-I3
sm-I2
sm-I1
InPort6
InPort5
InPort4
InPort3
InPort2
InPort1
12
12
12
13
13
13
12
12
12
1
IntakeManSpeed-1
7
6
5
4
3
2

Figure 3.5: Conversion of detailed intake manifold to a FRM with illustration of the reduced number of volumes.

Figure 3.5 illustrates the intake volume reduction where 23 flow volumes got reduced to a single flowsplit.

3.3.3 Calibration

The simplified subsystem need to be calibrated to insure the model predictability. For that purpose, the following parameters are usually considered: Heat Transfer Multiplier (HTM) and Friction Multiplier (FM) in pipes and flowsplits, while orifice diameter is tuned to calibrate the pressure drop. Two different approaches are used to evaluate the multipliers: Minimizing approach and Target approach.

3.3.3.1 Minimizing approach

$$\min\Big(|\Delta\dot{x}|\Big) = \{\Delta\dot{x} = \dot{x}_{sim}\Big(DIA \wedge HTM \wedge FM\Big) - \dot{x}_{exp}\} \tag{3.1}$$

$$, where:$$

$$\begin{cases} DIA = \Big[m, m+1, ..., n \text{ - } 1, n\Big] \\ HTM = \Big[i, i+1, ..., j \text{ - } 1, j\Big] \\ FM = \Big[i, i+1, ..., k \text{ - } 1, k\Big] \end{cases} , \begin{cases} \text{m = 50, n =110 [mm]} \\ \text{i = 0, j = 3 [1]} \\ \text{k = 5 [1]} \end{cases} \tag{3.2}$$

The minimization seen above is between simulation data and test cell measurement. In this first approach $\dot{x}_{sim}$ is the simulated property and $\dot{x}_{exp}$ is the measured value. It could be minimization of any property, including temperatures, pressures or massflows. $\dot{x}_{sim}$ is achieved through varying the tuning variables/parameters; the diameter (DIA), HTM and FM simultaneously. The typical ranges are also sorted, whereas the diameter varies between 50 and 100[mm]. HTM varies between 0 and 3, meaning the greater the number, the greater the heat transfer occur. Any value between 0 and 1 implies less heat transfer. The same applies to the FM, but within 0 and 5. These intervals are used unless it is stated differently.

3.3.3.2 Target approach

$$\text{Target}\Big(x_{exp}\Big),\ x_{sim}\Big(DIA \vee\ HTM \vee FM\Big) \rightarrow\ x_{exp}, x_{exp} = \Big[P \vee\ T\Big] \tag{3.3}$$

From hereon, either the diameter or the HTM or the FM is used, i.e. a single tuning variable is varied to match the measurements. The targets could be either pressure or temperature. x_{exp} is the engine test cell quantity and x_{sim} is the corresponding simulation value.

3.3.4 Validation

The FRM is run to validate the computational results against test cell measurement data. Figure 3.6 illustrates the change in the real-time factor after each subsystem simplification. It can be seen that the factor becomes lower after each volume reduction of every sub-system, meaning less computational time. The improvement in subsystem properties after calibration is herein exemplified by showing the results for turbine temperatures and pressures, see figure 3.7. It can be noticed that the properties are more aligned within the tolerances after the calibration step. Turbine temperatures are typically the most sensitive property and got affected the most.

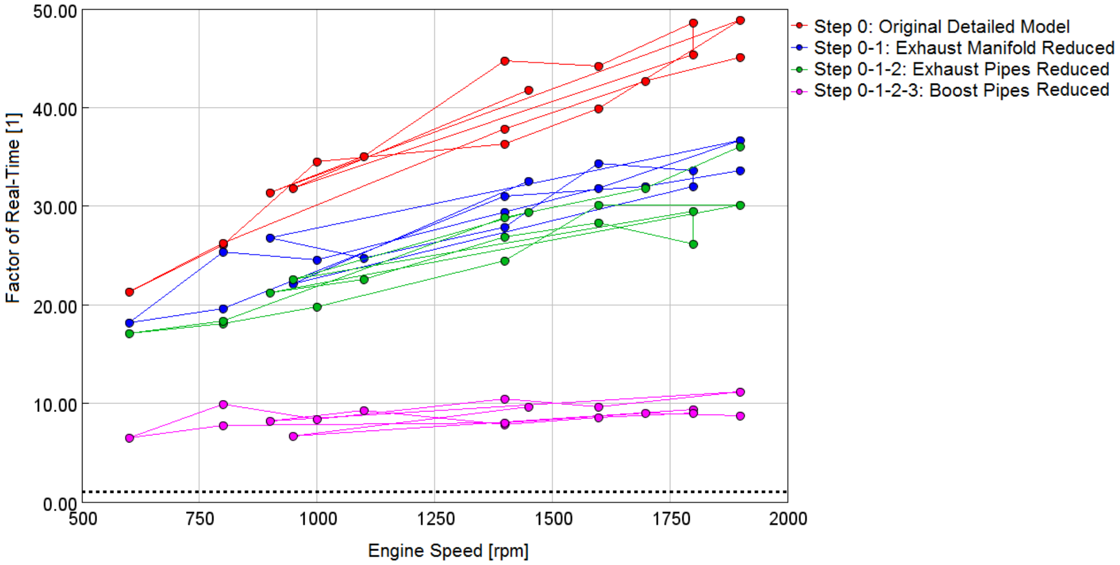

Figure 3.6: The change in Factor of Real-Time for each system reduced, one after the other.

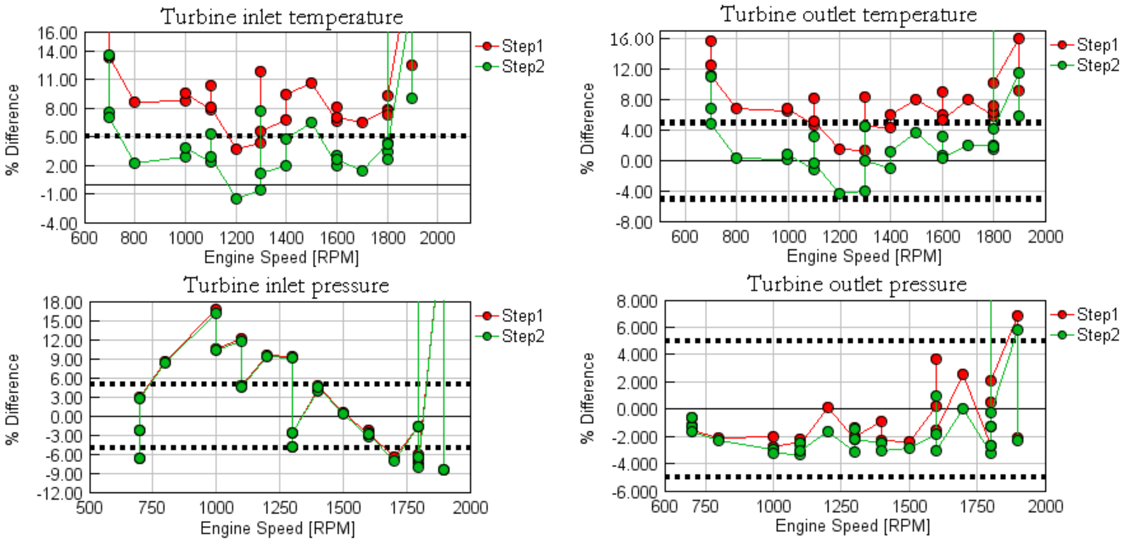

Figure 3.7: Turbine properties - Temperatures and pressure percent difference, inlet and outlet.

With the overall FRM process explained, the detailed simplification of each system or component will now be deduced in the following chapters, section 3.5.1-3.5.6. Although, a more thorough and theoretical explanation will firstly by provided for deeper understanding and will unveil how this benefits the simulation run speed.

3.4 Factor of Real-Time

The model delivered needs to be Real-Time (RT) capable, since the ECU environment in reality needs to take decisions equally fast or even faster. Evidently, RT is the actual time during an event or process occurs, with immediate response from the system observed. For example, if an event takes one minute in the engine test cell to occur, the same time duration has to be valid for the model as well. The HiL rig will also not function with a non Real-Time model, it will crash. Therefore, the RT will be frequently monitored during the FRM simulation process. Anything slower or faster than RT is referred to as a factor of RT and is a measure of how far away or close RT the process actually is. Hence, it is a direct property to observe where RT has a "Factor of RT" equal to one. If the process is slower, the "Factor of RT" will be greater than one. Obviously, a "Factor of RT" smaller than one can exist and means that the process occurs faster than RT. The process in this project is computational time for the engine model and how long that process occurs depends on the simulation run speed. Mentioning the run speed as the criteria to reach a FRM RT capable, there are three influencing factors: Machine hardware, machine software and model complexity. The latter one concerns the detailed model as the complexity is increased with the details included. Looking into model complexity, the following steps can be done to increase run speed and reach a RT FRM (3):

(i) Decrease the amount of calculations per time step. To achieve this, the total amount of sub-volumes (discretization) can be decreased by lower the number of cylinders or adjust the combustion model. Decreasing the amount of sub-volumes can be done through lumping volumes together. Then the calculation for one simulation time step will be for the lumped volume, instead of all individual branches of volumes and going through each one of them. The ability to predict combustion is especially important for transient conditions and for accurate numbers for emission levels. Less predictive model typically do not adjust according to different engine conditions for every operating point (same combustion profile for every case), has more imposed values, needs more experimental data, but is in turn faster. Hence, decreasing the number of cylinders take away the number of times the combustion profile needs to be determined.

(ii) Increasing time step size. Timestep size comes from sub-volume length through the “Courant Criterion” and also depends on the local flow velocity. Comparable is to have a less refined mesh, lower resolution. In the end, greater discretization length (sub-volume length), the greater time step and faster computation(3).

(i) decreasing the number of calculations per time step (fewer sub-volumes) and (ii) increasing the simulation time step size. If the time step is increased, meaning that the calculations are done with greater crank angles degrees in-between, the combustion profiles may change shape. If predictive combustion is a requirement, then sub-stepping can be done for the cylinder in order to capture it(3).

3.5 Detailed Conversion Procedure

This subsection describes the FRM conversion on the sub-system level. The conversion process started from the exhaust system with the highest velocities requiring short time steps. This means that, starting there would save the most computational time and the FRM process will go through faster.

3.5.1 Exhaust Manifold

3.5.1.1 Volume Reduction

It is important to note that the exhaust system has been split into two branches which enter the respective manifold of the twin scroll turbine. Thus, the system is tagged as two parts including the exhaust port volume, the runner volumes, the collector, the flowsplits volumes and the pipe volume. The simplified two-scroll exhaust manifold can be seen in figure 3.8 together with the detailed system.

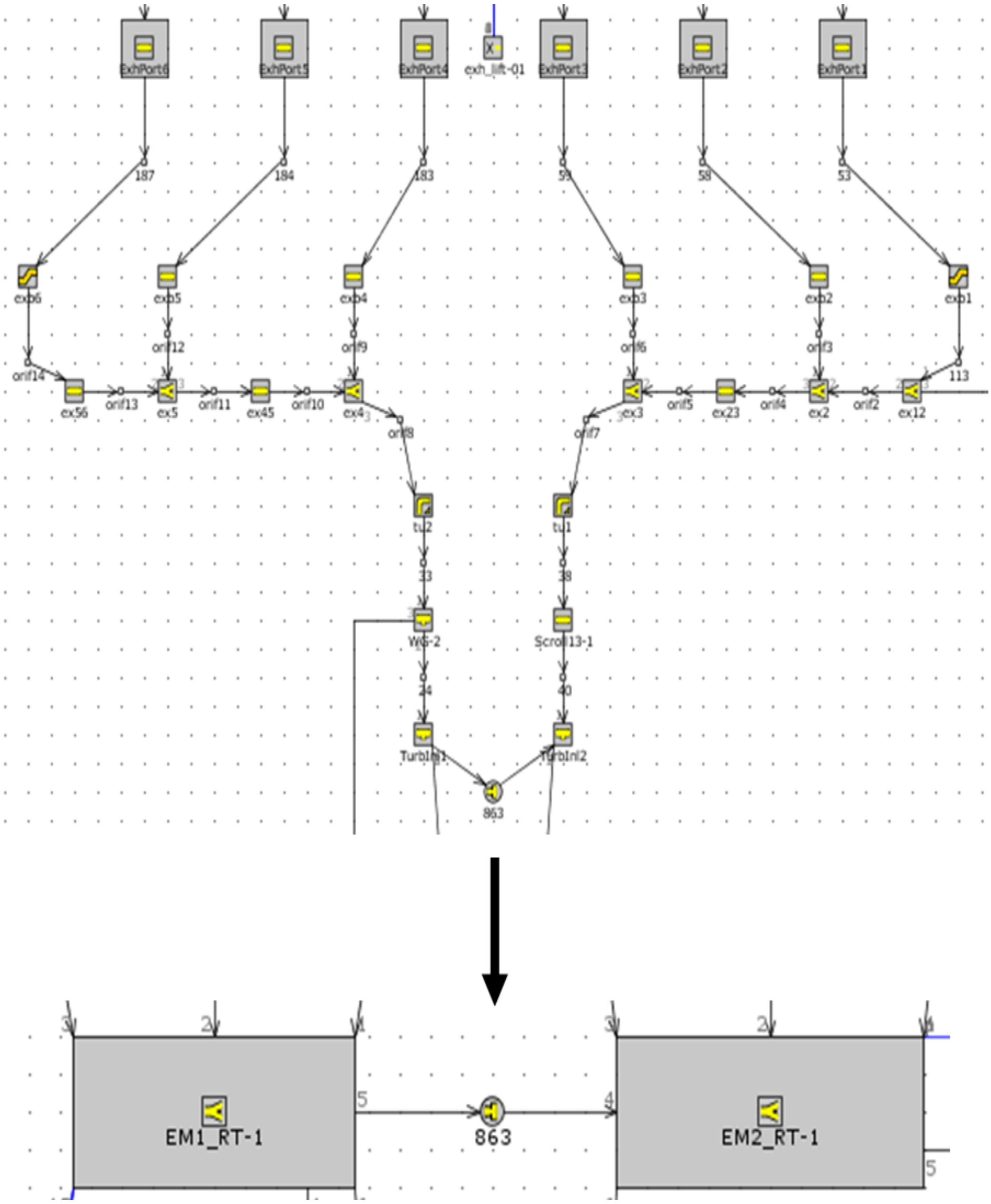
ExhPort6
ExhPort5
ExhPort4
exh_lift-01
ExhPort3
ExhPort2
ExhPort1
187
184
183
59
58
53
exb6
exb5
exb4
exb3
exb2
exb1
orif14
orif12
orif9
orif6
orif3
113
ex56
orif13
ex5
orif11
ex45
orif10
ex4
ex3
orif5
ex23
orif4
ex2
orif2
ex12
orif8
orif7
tu2
tu1
33
38
WG-2
Scroll3-1
24
40
TurbInl1
TurbInl2
863
EM1_RT-1
863
EM2_RT-1

Figure 3.8: The reduction step of volumes for the exhaust manifold sub-system.

3.5.1.2 Calibration

Minimizing and targeting approach were both tested, and the one that performed better was used for a given subsystem. The approaches tried to calibrate the turbine inlet temperatures. Either varying the HTM and FM, or only varying the HTM is recommended.

3.5.2 Exhaust Pipes

3.5.2.1 Volume Reduction

The exhaust pipes comes after the turbine and compressor shaft. It consists of the Exhaust After Treatment System (EATS) and the output end pipes. It contains mostly straight pipes and flowsplits volumes. The EATS is an extensive package with a significant amount of volumes. Thus, adopting this system simplification early in the FRM process will help the FRM conversion duration for the better. The transformation can be observed in figure 3.9 leaving only two volumes, a flowsplit and a bell-mouth respectively.

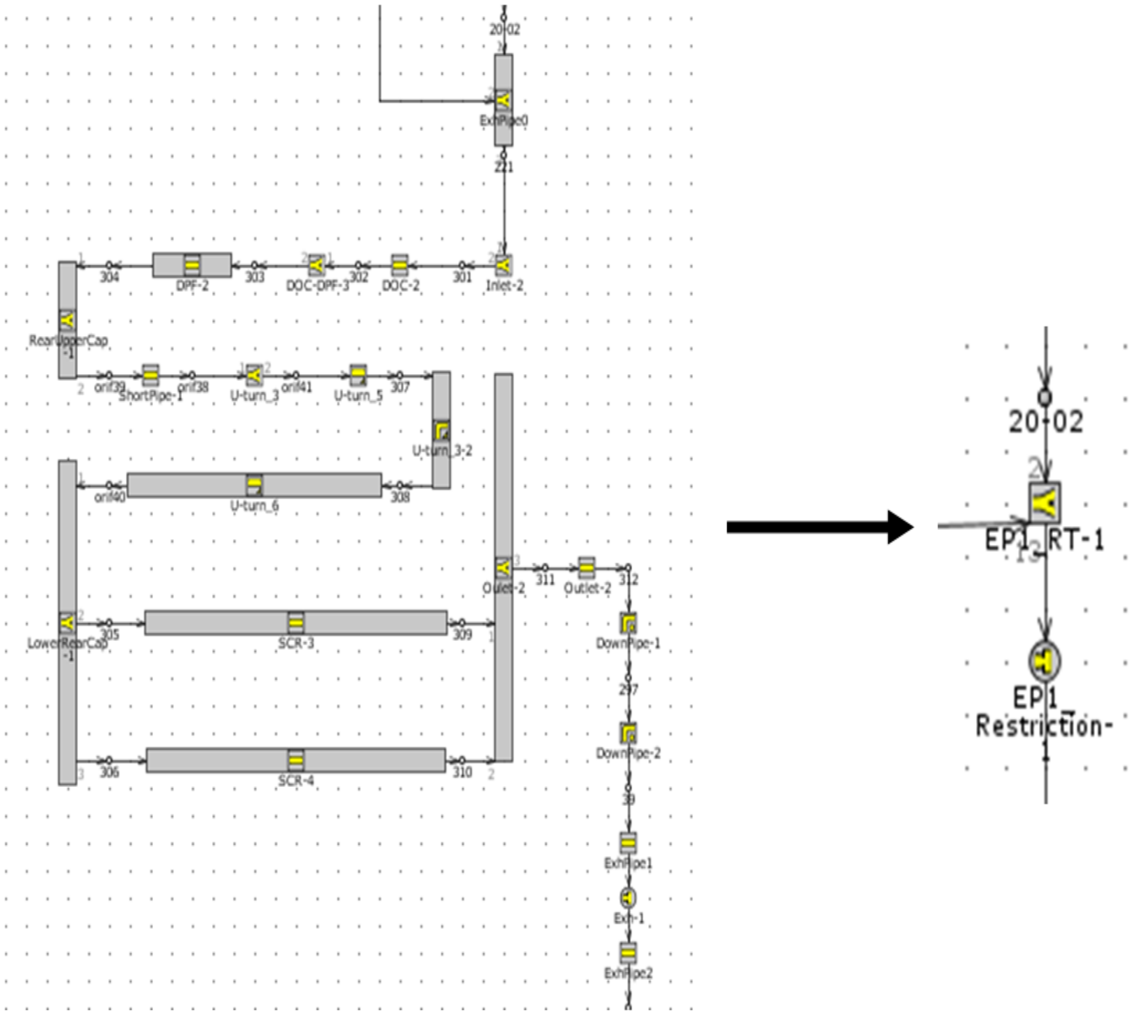
20-02
ExhPipe0
221
Inlet-2
301
DOC-2
302
DOC-DPF-3
303
DPF-2
304
RearUpperCap-1
orif39
ShortPipe-1
orif38
U-turn_3
orif41
U-turn_5
307
U-turn_3-2
308
U-turn_6
orif40
Outlet-2
311
Outlet-2
312
LowerRearCap-1
305
SCR-3
309
306
SCR-4
310
DownPipe-1
297
DownPipe-2
39
ExhPipe1
Exh-1
ExhPipe2
20-02
EP1_RT-1
EP1_Restriction-

Figure 3.9: The reduction step of volumes for the exhaust pipes´ sub-system.

3.5.2.2 Calibration

Though multiple approaches can be used, targeting exhaust pressure was performed by varying the orifice diameter.

3.5.3 EGR Pipes

3.5.3.1 Volume Reduction

The EGR circuit comes after the exhaust manifold and reconnect to the intake pipes via the EGR mixer just before the intake manifold. The result is three volumes, namely a flowsplit, a bellmouth and a pipe. The simplification can be seen in figure 3.10.

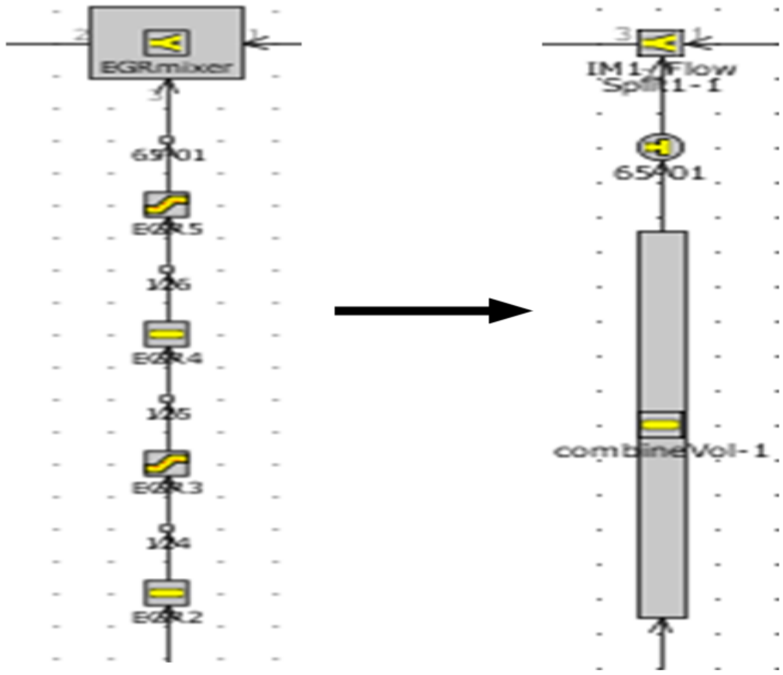

Figure 3.10: The reduction step of volumes for the EGR pipes´ sub-system.

3.5.3.2 Calibration

For a real-time model, the maps has to be updated. Subsequently, throttle angle or valve lift is calibrated to match measurements of CO2 mole fraction and then an EMS signal has to be fitted using a trend line.

3.5.4 Boost Pipes

3.5.4.1 Volume Reduction

The boost pipes is another extensive subsystem and computational heavy due to all the volumes. It starts after the compressor and continues to the CAC-throttle, just before the EGR-mixing. The simplification results in for volumes, where the heat exchange, cooling of the charge is still simulated after the simplification. The reduction process can be seen in figure 3.11.

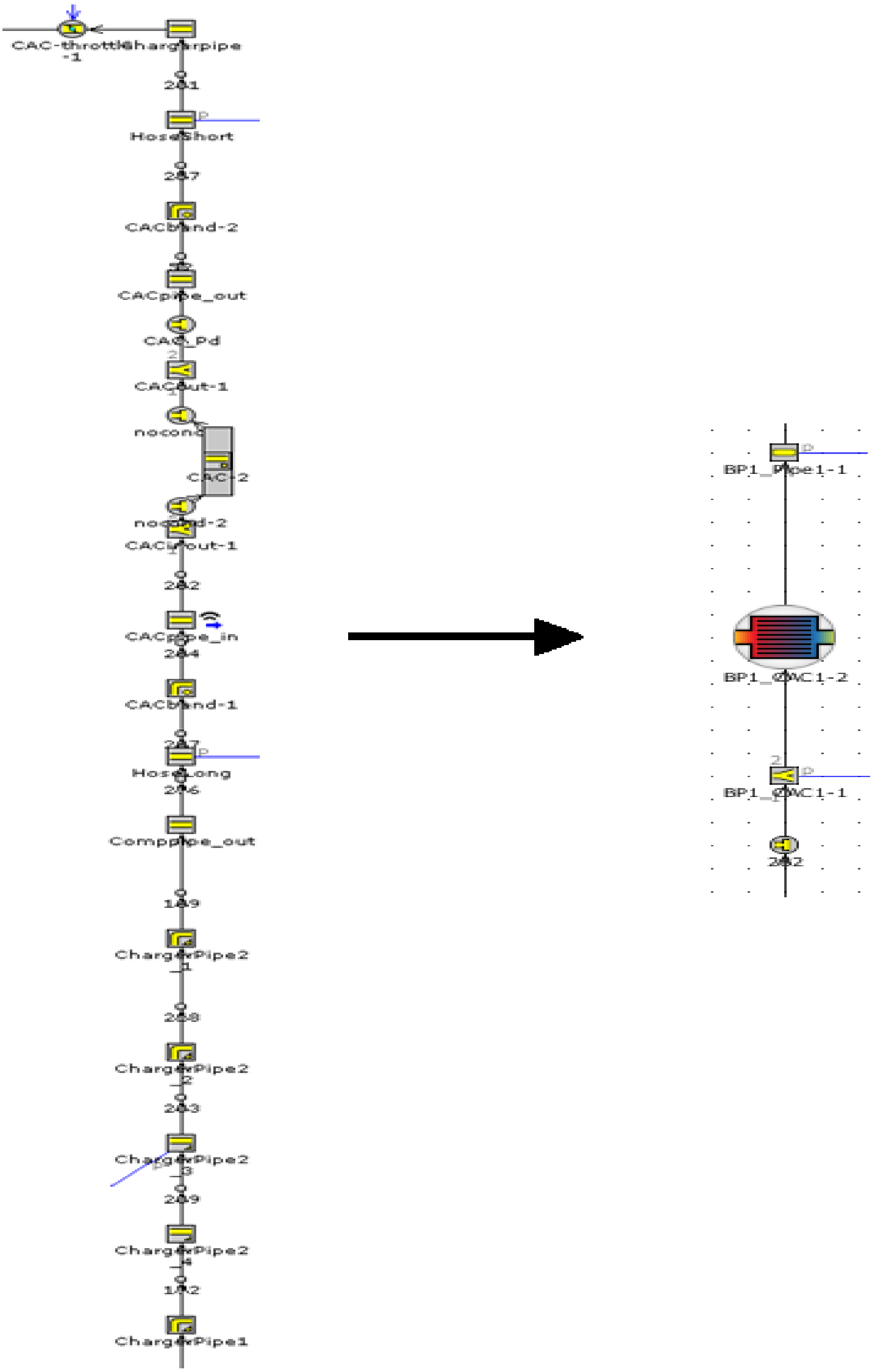
CAC-throttle-1
Chargerpipe
241
HoseShort
247
CACbend-2
CACpipe_out
CAC_Pd
CACout-1
nocond
CAC-2
nocond-2
CACinout-1
242
CACpipe_in
244
CACbend-1
HoseLong
246
Comppipe_out
149
ChargerPipe2_1
248
ChargerPipe2_2
243
ChargerPipe2_3
249
ChargerPipe2_4
142
ChargerPipe1
BP1_Pipe1-1
BP1_CAC1-2
BP1_CAC1-1
242

Figure 3.11: The reduction step of volumes for the boost pipes´ sub-system.

3.5.4.2 Calibration

In this step, the minimization approach is used, with respect to air massflow. The diameter is varied between 45[mm] and 75[mm] together with the HTM and FM tuning parameters.

3.5.5 Intake Manifold

3.5.5.1 Volume Reduction

The intake manifold comes after the EGR-mixer and goes to the straight six cylinder bank via the ports. The reduction leaves two volumes behind where one flowsplit represent the whole manifold basically. The reduction can be seen in figure 3.12.

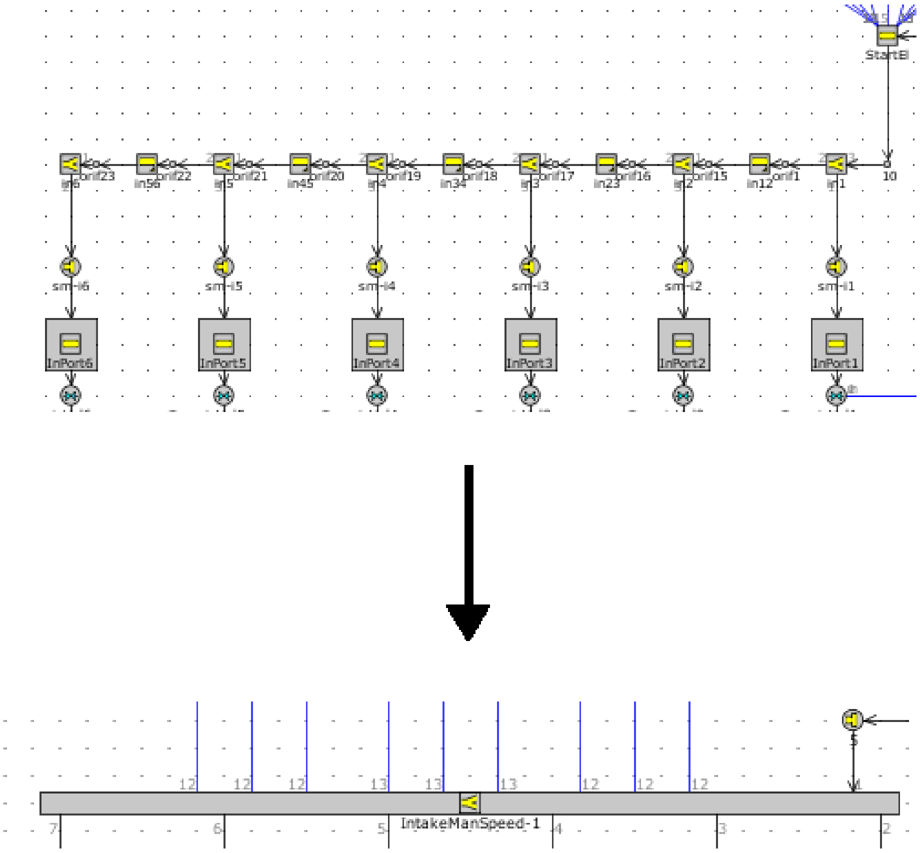
StartBl
orif23
lin56
orif22
orif21
lin45
orif20
orif19
lin34
orif18
orif17
lin23
orif16
orif15
lin12
orif1
10
sm-i6
sm-i5
sm-i4
sm-i3
sm-i2
sm-i1
InPort6
InPort5
InPort4
InPort3
InPort2
InPort1
12
12
12
13
13
13
12
12
12
IntakeManSpeed-1
7
6
5
4
3
2

Figure 3.12: The reduction step of volumes for the intake manifold sub-system.

3.5.5.2 Calibration

In case of the intake manifold, targeting the compressor outlet pressures by varying the HTM is the recommended approach.

3.5.6 Intake Pipes

3.5.6.1 Volume Reduction

The intake pipe subsystem set the first diameter on the engine´s cold side with the bell-mouth. The other volumes before the reduction are an air-filter and the very special compressor inlet volume. In the end, the reduction can be captured in figure 3.13.

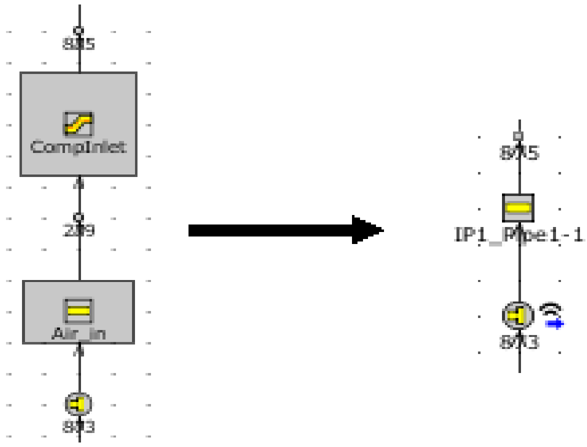

Figure 3.13: The reduction step of volumes for the intake pipes´ sub-system.

3.5.6.2 Calibration

In this step, the diameter of the pipe is varied between 70mm and 120mm to achieve the measured compressor inlet pressure. The calibration approach is targeting and the calibration point used is with respect to the maximum airflow. If nothing else is stated, the maximum airflow point will always be used for calibration.

4

Results and Discussion

The resulting graphs and figures need some preliminary explanations since the same structure is used throughout the chapter. The tolerances are limits driven by Volvo Penta as their industry standard about which levels of percent differences (errors) between simulation and experiment values are acceptable. The experimental values come from a PLM run from the engine test cell. The percent difference is given by $\frac{X_{Sim}-X_{Exp}}{X_{Exp}}$, where X_{Sim} and X_{Exp} represent simulation and experimental values, respectively. The result of this calculation is referred to as Difference [%]. Pressures and temperatures have tolerances of 5% and airflow rate 3%. Pressures and temperatures are from the compressor and the turbine inlets and outlets, the airflow rate is for the cold side of the engine.

4.1 The Final FRM Model

The main findings presented in this section concern simulation run speed and results for the compressor and turbine pressure and temperatures, as well as the airflow rate. In addition, best calibration practice is discussed.

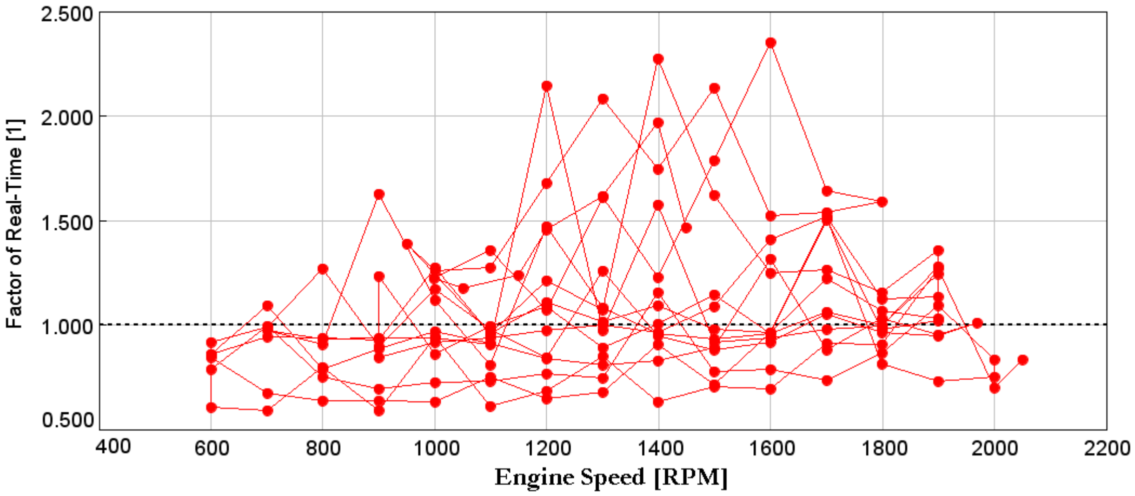

Figure 4.1: The final Factor of Real-Time accomplished for the FRM model

In figure 4.1 above the final Factor of Real-Time can be observed for all the simulated cases. The end result was the average factor of real-time of 1.07. For comparison, the average factor of real-time for the detailed model was 39.4. The FRM reached Real-Time with a Factor of Real-Time close enough to 1, with a predictive combustion model. Hence, the model fulfills the real-time prerequisite to be used in a HiL environment.

4.1.2 Timestep Angle

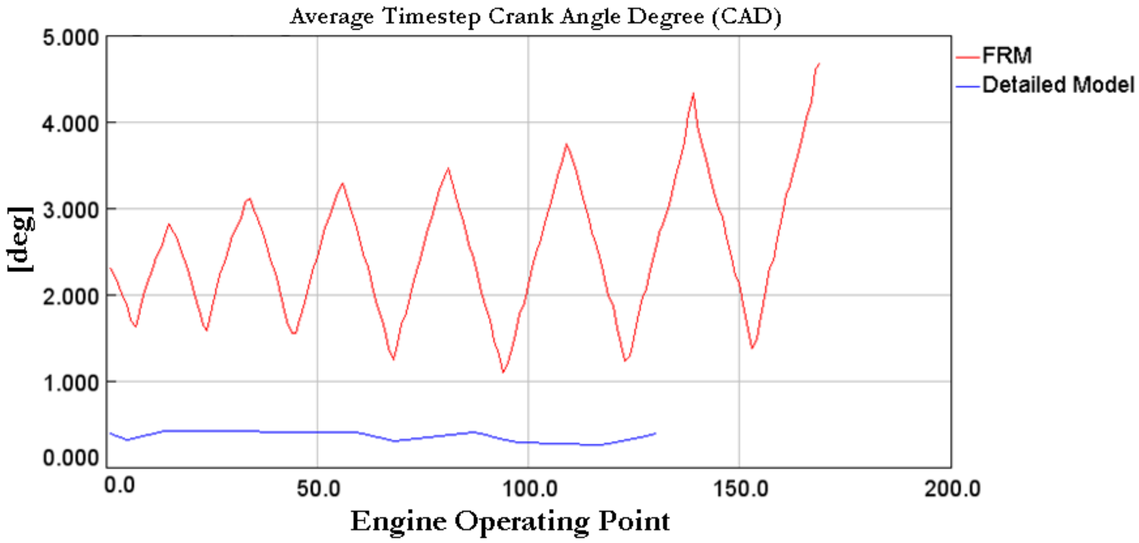

Figure 4.2: The resulting time step in CAD for both detailed model and FRM.

In figure 4.2 the crank angle degree (CAD) resolution is shown for all PLM points for both detailed model and FRM. The purpose is to show how much the crank angle degree increase between every other calculation in the volumes. It is expected to increase in comparison to the detailed model which is visualized. The pattern of the CAD also follows the engine test cell speed and load sweep, i.e. the observed trend is not noise. The timestep is after all flow velocity dependent, locally. Following the Courant criteria as the explicit solver is used, higher local velocities implies smaller crank angle timestep for numerical stability. As the local velocity $\frac{\Delta x}{\Delta t}$ increase and discretization length Δx is the same, the crank angle timestep Δt needs to be refined in order for the Courant criteria to hold. For the detailed model the timestep in CAD is was always below 1. It was possible to increase this CAD step in the FRM and hence increase the model run speed.

4.1.3 Compressor and Turbine Temperatures

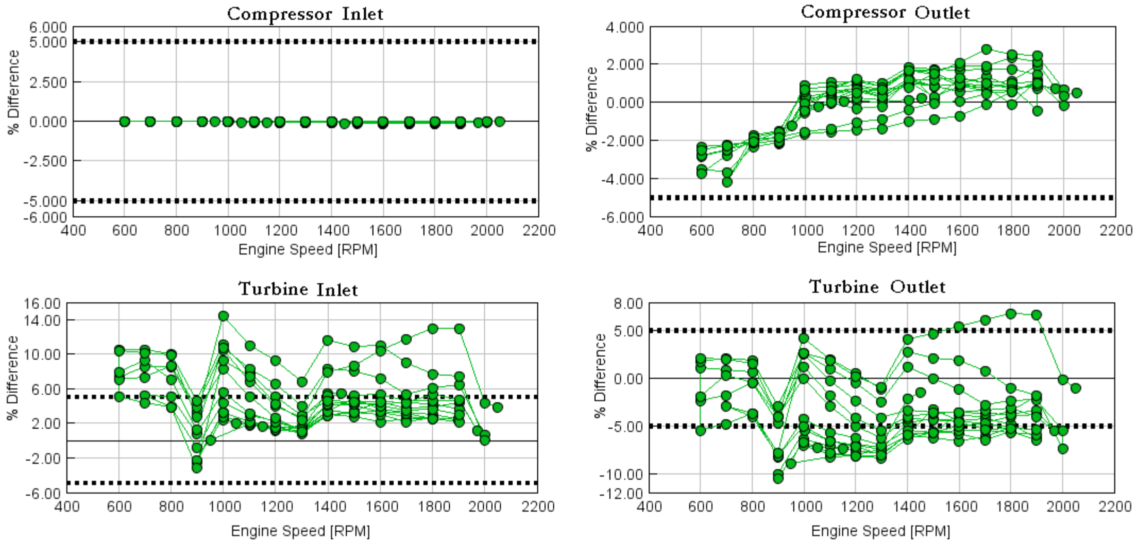

Figure 4.3: The percent difference for compressor and turbine temperatures, inlets and outlets.

In figure 4.3, the final percent difference for compressor and turbine inlet and outlet temperatures can be observed. The purpose is to show the difference between the FRM simulated results and the measurement data. Note that the compressor inlet temperature has been imposed in the model. Compressor outlet temperature difference is entirely within the 5% limit. Compressor properties have been easier to calibrate in comparison to the turbine properties. The hot side of the engine in general has been more demanding to calibrate and this can be due to more unsteady flow and greater velocities. Another reason could be errors being accumulated and pushed further downstream in the model and coming to expression in the very last components, e.g. the turbine. The turbine inlet as seen in the graph could have been better of course, nevertheless the majority of the engine points are still within the 5% limit. The turbine inlet properties, temperature and pressure, have been the hardest to predict within the tolerances. Even after re-calibration to enhance their predictions, there is often a trade-off. This trade-off is typically expressed the strongest between the turbine inlet and outlet properties, meaning that if the inlet properties are enhanced, the outlet get worse and vice versa. It also leads to the conclusion that the turbine inlet properties were sacrificed to a certain extent in order to enhance other component properties and that this trade-off was the most beneficial in overall for the model predictive capability. To conclude the FRM model´s prediction ability of the turbine temperatures, the inlet and outlet are overestimated and underestimated respectively. Another pattern observed is that if the mentioned overestimation is mitigated, the underestimation typically get magnified proportionally. Considering this statement, the ultimate over- and underestimation relation is more or less achieved. Meaning, the underestimation is in the same magnitude as the overestimation.

4.1.4 Compressor and Turbine Pressures

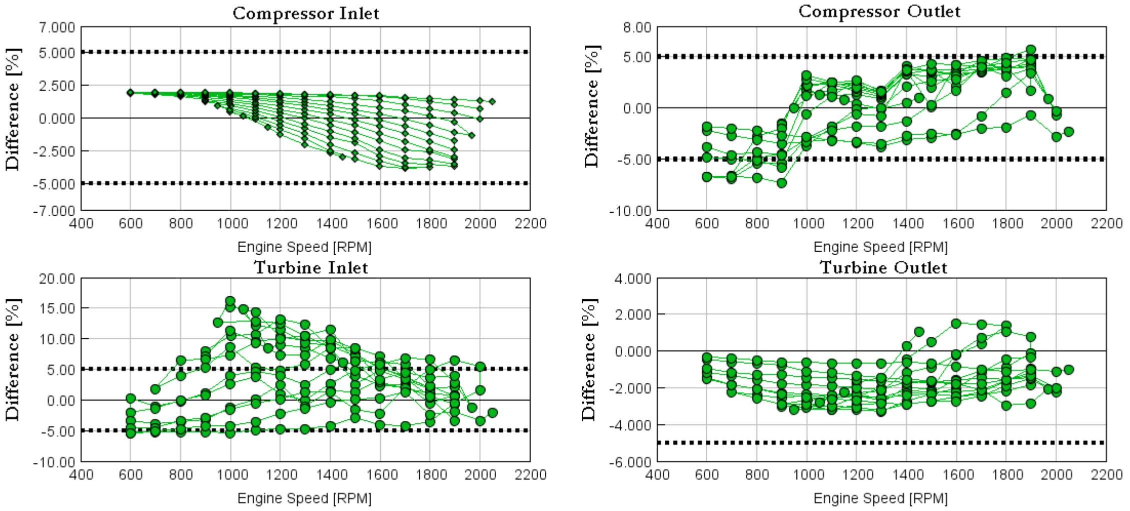

Figure 4.4: The percent difference for compressor and turbine pressures, inlets and outlets.

In figure 4.4, the final percent difference for compressor and turbine inlets and outlets pressures can be observed. The compressor inlet and outlet result can be seen in the upper figures, left and right, respectively. Looking at all graphs, it can strongly be motivated that the result is really proper and within the tolerances given. The pressures look far better than the temperatures described previously. This is due to the trade-off discussed for the temperatures. However, once again the turbine inlet pressures could ideally have been better looking. Preferably, the turbine outlet could have been worsened to enhance the inlet as described previously with the temperatures. This relation is not always possible to realize since the outcome also depends on other predicted properties, e.g. the airflow rate. The red line crossing appear at engine operating point hundred, giving 100 [mg] of injected fuel mass, anything beyond that operating point has less injected fuel mass and lower load. With that enlightened knowledge, the graphs can be analyzed further in detail.

4.1.5 Airflow Rate

In figure 4.5 the airflow rate percent difference is presented. The vertical dotted red line shows where the low engine load starts and has importance when discussing the results. The importance of the data observed, the engine points, are discussed in great detail in chapter 3.2.1. In short terms, the greater loads are of more interest since those are the typical engine operating points. Low loads for the D13 Volvo Penta engine are typically around less than 100 [mg] of the injected fuel mass, giving BMEPs (Brake Mean Effective Pressures) of 6-8 [bar] or 600-750 [Nm] of torque. The airflow percent difference is seen to be within a 5% limit at least, i.e. before the low loads starts. Beyond the engine point for the start of low loads, the percent difference have escalated in magnitude. However, the important operating range leaves satisfactory results, considering the first part of the graph with greater loads.

The mean value for those engine operating points percent difference comes below 3% which was the tolerance limit.

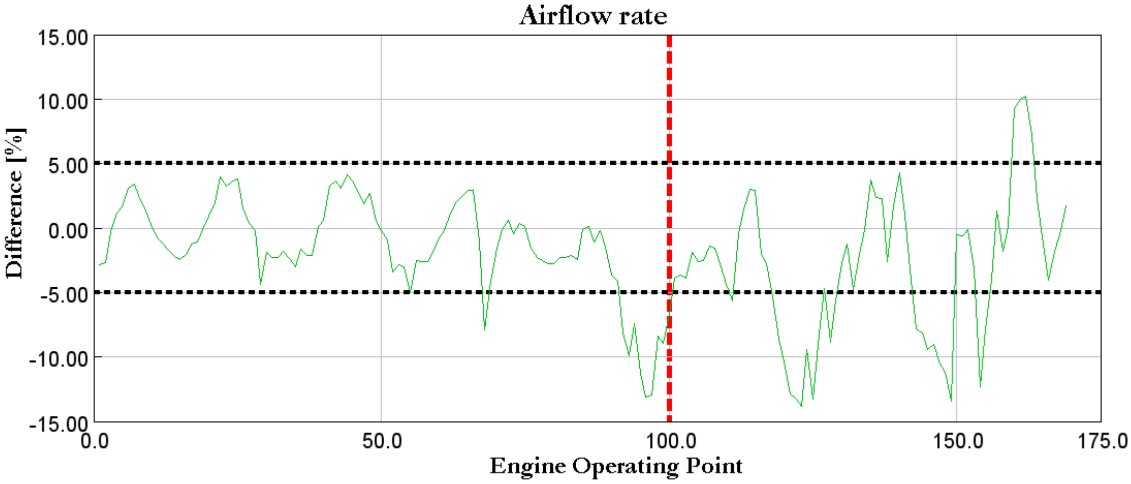

Figure 4.5: The resulting percent difference for the airflow rate.

4.2 Best calibration practice

In this section the best calibration practice will be explained thoroughly for all the sub-systems of the engine model: Intake pipes, boost pipes (CAC), intake manifold, exhaust manifold and exhaust manifold. Before one sub-system calibration starts, a few considerations need to be made regarding how the calibration should be performed since there are different alternatives to choose from. Firstly, the computational method needs to be determined - should the calibration process make use of targeting or minimization? Targeting is where simulation absolute property values are compared with reference data (herein the PLM data). Minimization is a mathematical method to minimize the difference between simulation and experiment data. Which engine operating points should be used for calibration and bench-marking? In this project, either maximum airflow or maximum engine speed operating point were considered. In summary, these three questions need to be addressed before calibration:

I] Which calibration point to use, maximum airflow or maximum engine speed?
II] Which calibration approach to use, targeting or minimizing?
III] Which property to calibrate against: Pressure or temperature, compressor or turbine, inlet or outlet? Or simply massflow?

What makes it more complex is the fact that there are many combinations possible within I]-III] and that is why the investigation is desirable. Which combination of I]-III] is the most appropriate one for a specific sub-system calibration?

Figure labelling:
The figure labels for this chapter need a separate nomenclature explanation:

Min(dP) - Minimizing the pressure difference, compressor or turbine, inlet or outlet.
Min(dT) - Minimizing the temperature difference, compressor or turbine, inlet or outlet.
Min(mdot) - Minimizing the airflow rate difference on the cold side.
Target(Pexh) - Targeting exhaust pressure, upstream the turbine.
Max RPM - Using maximum engine speed as calibration point.
Max air - Using maximum engine airflow rate as calibration point.
Reference - A previous non-calibrated state of values and properties.

Properties used for each calibrated system:
The labelling in the figures change meaning depending on which sub-system that is discussed, it depends on the location in the engine model. The closest located property (of compressor or turbine) to the system up for calibration will be used because that gives the most accurate calibration:

Intake Pipes - Compressor inlet pressure.
Boost Pipes - Compressor outlet pressure.
Exhaust Manifold - Turbine inlet temperature or pressure.
Exhaust Pipes - Turbine outlet temperature or pressure.

To be noted:
Temperatures are not used for calibration property on the cold side. If massflow is used, it is always from the same location; engine´s cold side, intake pipes, regardless of sub-system calibrated. Thus, the massflow should be the same in every location in the model and in reality (mass conservation).

4.2.1 Intake Pipes

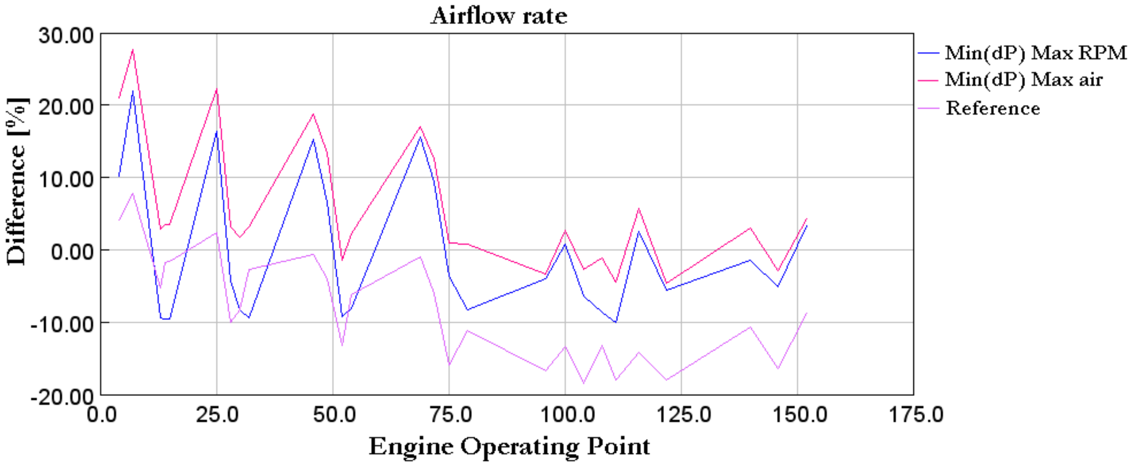

Figure 4.6: Calibration results for airflow rate using two calibration points maximum airflow and maximum engine speed.

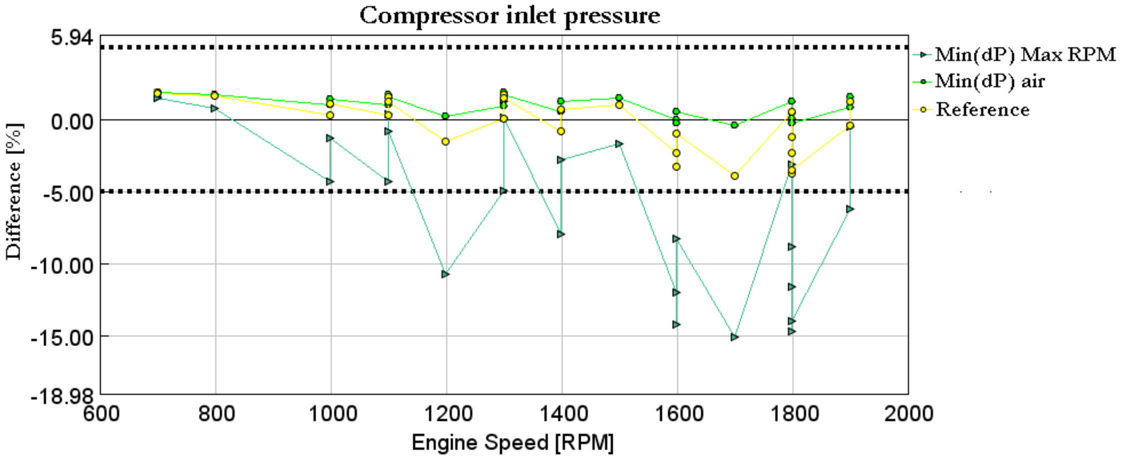

Figure 4.7: Calibration result for compressor inlet pressure using two calibration points: maximum airflow and maximum engine speed.

Figure 4.6 shows that both calibration points (maximum air flow and maximum engine speed) provide rather similar results for predicting air flow rate. However, the results for the compressor inlet pressure (see figure 4.7) show that the maximum airflow calibration point is the better choice. In addition, both minimizing and targeting calibration approaches provide satisfactory results. Although, using minimization as approach may not settle for one solution. For example, if the upper limit is increased for the tuning parameters (DIA, HTM and FM) for the range of calibration, the diameter will always end up with the greatest diameter for the given interval. That is expected since it is a minimization approach, it will always settle for a solution within the given interval and when checking other intervals the solution will most likely be another one. The person performing the calibration using minimization as approach has to be aware of this implication. In this scenario, experience would contribute a lot. The choice of calibration approach will is not of significance for this sub-system. Nevertheless, using another property than compressor inlet pressure was not possible, result became unreasonable.

4.2.2 Boost Pipes

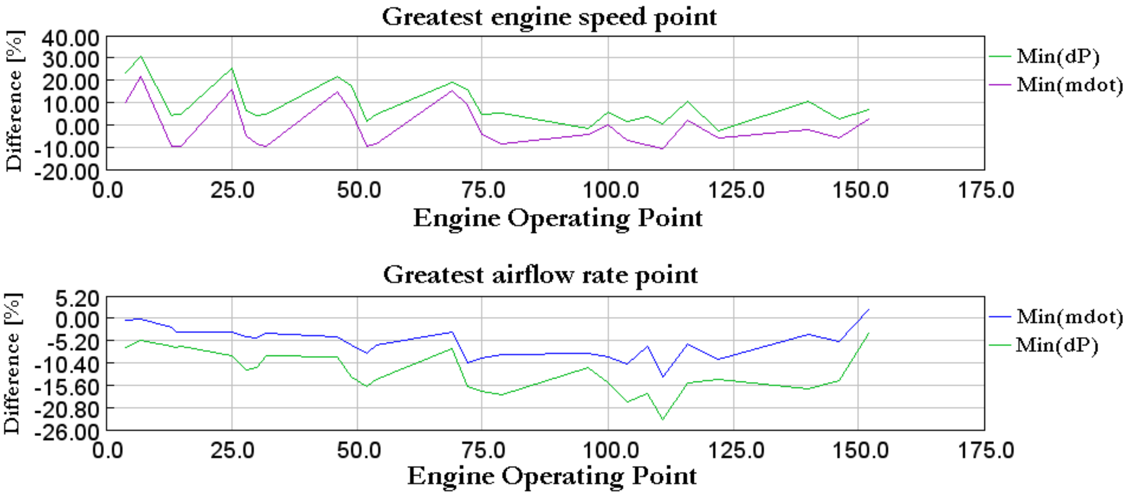

Figure 4.8: Boost Pipes - Pressure and massflow minimization approach, using max engine speed and max airflow as calibration points.

The results shown in figure 4.8 concern the compressor outlet pressure and air massflow. It is seen that using maximum airflow calibration point to minimize air massflow provides the best alignment with measurement data. It should be noted that targeting massflow approach lead to convergence issues. Usually, the compressor outlet pressure is the calibration property and not the massflow. Thus, targeting approach can be used if the compressor outlet pressure is targeted but it is not recommended as the primary calibration approach.

4.2.3 Exhaust Manifold

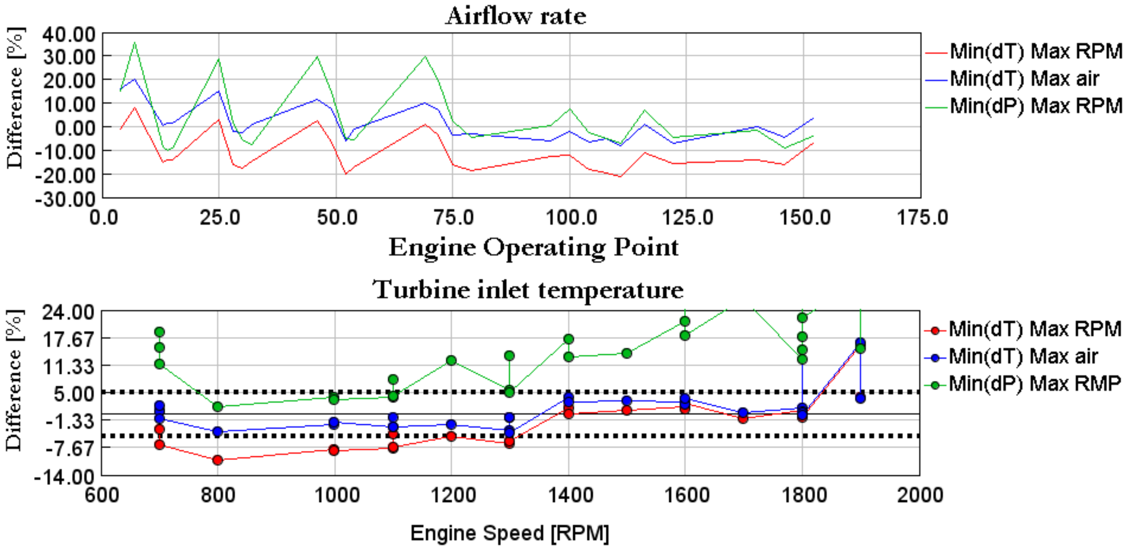

Figure 4.9: Exhaust Manifold - Minimizing pressure and temperature difference, using max engine speed and airflow as calibration points.

Figure 4.9 shows that the approach for calibrating the exhaust manifold temperature is to minimizing the turbine inlet temperature using the maximum airflow point for calibration.Targeting approach works equally well (not shown herein). Minimizing approach makes it possible to vary three variables (diameter, HTM, FM) contrary to targeting approach when only one variable can be varied. With that in mind, minimizing approach provides better possibility for accurate calibration. Therefore, minimizing approach seems to be preferable approach. However, the upcoming subsystem "Exhaust Pipes" will reveal that this is not the case for all subsystems.

4.2.4 Exhaust Pipes

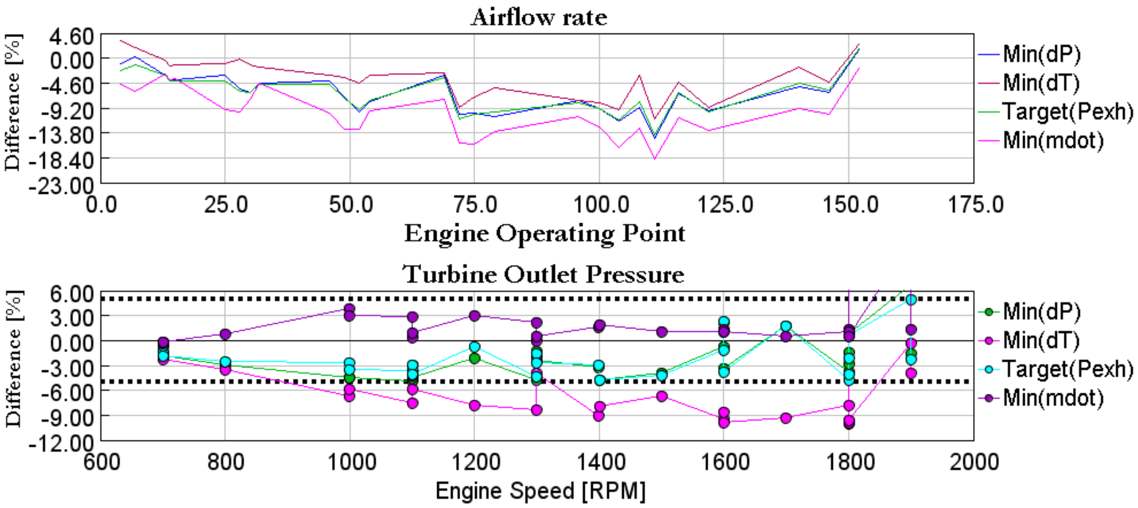

Figure 4.10: Exhaust Pipes - Airflow rate and turbine outlet pressure percentage difference, using maximum airflow point for calibration.

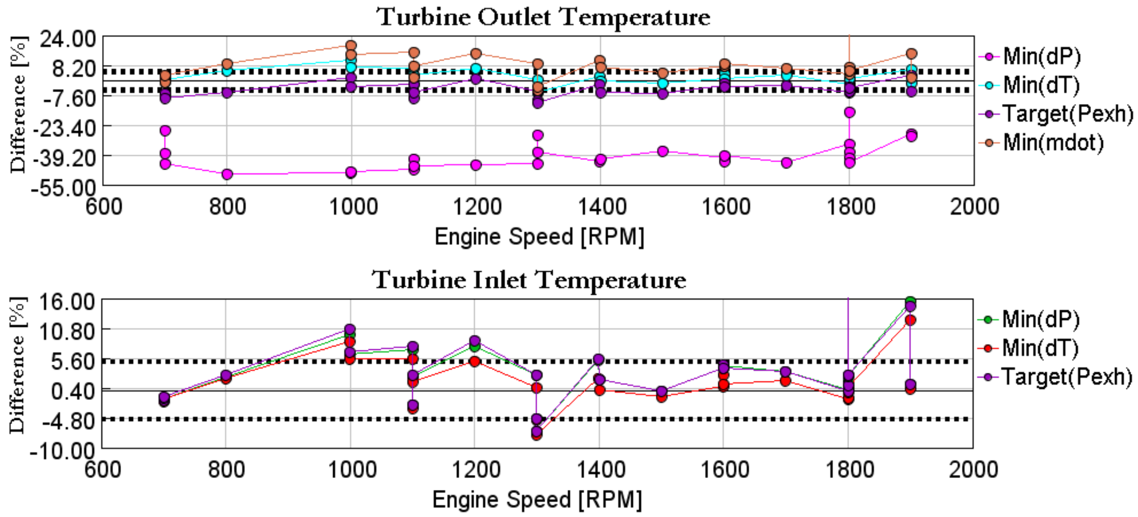

Figure 4.11: Exhaust Pipes - Turbine inlet and outlet temperature percentage difference, using maximum airflow point for calibration.

The calibration of the exhaust system, concerns properties downstream the turbine. The results in figures 4.10 and 4.11 are obtained for maximum airflow calibration point. The simulations did not converge when using maximum engine speed calibration point. Figure 4.10 shows that minimizing the airflow is not good calibration approach. The same figure illustrates that minimizing the temperature should not be considered for turbine outlet pressure calibration. When analyzing the turbine temperatures in figure 4.11, minimizing the exhaust pressure results in unacceptable differences between simulated and measured data. Therefore, targeting the exhaust pressure using maximum airflow emerges as the best choice. Moreover, as in the most calibration runs performed, it becomes the matter of reaching trade-off for the turbine properties since it always happens that one of them will be out of the tolerance range. One example is shown in figure 4.11 for the turbine inlet temperatures. The targeting approach was chosen as the primary calibration approach, but the turbine inlet temperature predictions are worse compared to any other calibration approach available. If these properties are under the process of improvement, decreasing turbine inlet temperature percentage difference usually worsens the outlet temperature and vice versa. If the previous statement unlikely does not hold, some other property will not be predicted with sufficient accuracy. Most likely airflow, which is of greater hierarchy and will thereof not be sacrificed.

4.2.5 Comments

The purpose of the results presented in this chapter is to motivate the best calibration practice and to exclude non-suitable calibration approaches for every sub-system. The exact choice of pressures and temperatures for the calibration approach depends on how close the sub-system is to the turbine and compressor inlet and outlet locations. For example, the sub-system exhaust manifold is the closest to the turbine inlet, and both temperature and pressure were investigated. It is done in this manner since this give more accurate calibration result and makes more sense rather than choosing two systems offset from each other. For example, calibrating the exhaust manifold multipliers by targeting the intercooler massflow, which would be non-intuitive. Absolute percentages graphs could have been used to only display the error percentage between simulation and measurements. However, if both positive and negative percentages are present, the model performance trend can be monitored. Positive and negative percentages giving trends towards over- and underestimation, respectively. Another important remark is that the sub-systems investigated are dependent on each other and earlier calibrations performed, meaning that different choices in calibration procedure would lead to different results.

5

Conclusions and Future Work

The aim of this thesis is to build a real-time capable high fidelity engine model to be used in HiL applications in virtual testing. The engine under consideration is the D13-700 Volvo Penta heavy-duty diesel engine. The focus of the work was to create a GT-SUITE Fast Running Model (FRM) using the detailed engine model and Part Load Map (PLM) data.

The detailed description of the detailed model - FRM conversion process is described in Chapter 3.5. The discussion includes the choice of the sub-systems, the geometry simplification, and the calibration procedure. The created FRM, which uses a predictive combustion model, is capable to run in real-time on the HiL system. The crank angle degree (CAD) for which the combustion is predicted is flow velocity dependent and it follows a zig-zag pattern through a speed-load sweep.

The gas-flow path was calibrated using the highest mass flow rate operating point. The predicted massflow rate was within specified tolerances for high loads, which are typical engine operating points. The intake pipes were calibrated using targeting approach for the compressor inlet pressure. Charge Air Cooler (CAC) was calibrated using minimizing approach for the massflow rate. The calibration of the intake manifold was carried out by targeting compressor outlet pressures. Moreover, for the exhaust manifold both minimizing and targeting approaches for turbine inlet temperature proved to be useful. Finally, the exhaust pipes can be calibrated effectively targeting the exhaust gas pressure.

Regarding the recommendation for future work, one important aspect to consider is improving the calibration practice by using advanced optimization tool which can vary multiple parameters to achieve the given target. Another possibility would be to explore and investigate additional calibration approaches where multiple subsystems are calibrated simultaneously. Moreover, improvement of the accuracy of the static maps used in the FRM is highly important for HiL applications. Further adjustment of measurement sensor locations needs to be considered as well to provide better fit with the corresponding location in the base model. The model need to be tested and further calibrated for transient operating conditions, using for instance Non-Road Transient Cycle (NRTC).

Finally, the best practice recommendation for the future FRM re-calibration is provided.

If the calibration is performed for the first time, the subsystems should be calibrated in the following order:

1. Exhaust Manifold
2. Exhaust Pipes
3. Boost Pipes
4. EGR Pipes
5. Intake Manifold
6. Intake Pipes

If re-calibrating, the following steps should be undertaken:

1. Update maps
2. Boost Pipes
3. Exhaust Manifold
4. Exhaust Pipes

Bibliography

[1] Charlton, S.J.C., 2005, ‘Developing Diesel Engines to Meet Ultra-low Emission Standards’, Cummins, Cummins Inc., Rosemont/Illinois/USA, pp. 7-11.

[2] P. J. Shayler & A. J. Allen, PJS & AJA, 2005, Running Real-Time Engine Model Simulation with Hardware-in-the-Loop for Diesel Engine Development, Roberts, Jaguar Cars Ltd., Detroit/Michigan/USA, pp. 1-2.

Gamma Technology PDFs:

[3] Daniel Schimmel, D.S., 2017, ‘GT-POWER FRM Training’, from Gamma Technologies (GT) FRM training course.

[4] GT‘s Engine Performance Application Manual (2017) p.26-29, p.37-40, p.45-46, p.52-53, p.59-61, p.114.

[5] GT´s Flow Theory Manual (2017) p.1-8, p.36, p.62.

Books:

[6] John B. Heywood, J.B.H., 1988. Internal Combustion Engine Fundamentals. New Work St. Louis San Francisco Auckland Bogotá Caracas Lisbon London Madrid Mexico City Milan Montreal New Delhi San Juan Singapore Sydney Tokyo and Toronto: McGraw-Hill, Inc. pp. 25-41.

[7] Frank M. White. 2011. FLUID MECHANICS. 7th ed. New York: The McGraw-Hill Companies, Inc. Chapter 3, pp. 143-199.

[8] Richard Stone, R.S., 1992. 2nd ed. Introduction to Internal Combustion Engines. Hampshire and London: The Macmillan press LTD. pp. 121–175.

Lectures:

[9] Karlsson, S. (2016). Electrification of the transport with a focus on cars.

Internet:

[10] http://ec.europa.eu/environment/air/transport/road.htm, date; 2017-05-12, time; 12:11 p.m.

[11] `http://www.volvopenta.com/volvopenta/na/en-us/our_company/press_releases/_layouts/CWP.Internet.VolvoCom/NewsItem.aspx?News.ItemId=8709,` `date; 20170512, time; 12:37 p.m.`

A

Appendix

A.1 Governing Equations Derivation

The laws of mechanics are written for one defined system, one fixed mass. These laws specify what happens when the defined system interact with its surroundings, where the boundaries separates the externalities and the system. The system approach let us establish a dynamic mechanical analysis of the environment. With that spirit in mind, fluids in motion (fluid dynamics) can also be studied by converting a system analysis to a control volume analysis. In fluid dynamics, specific regions are the subject of matter rather than individual masses and the system particles only occupy the laws for only an instant, until the next system of particles arrive. There is a need of converting the basic mechanical system laws to a control volume approach. Reynolds Transport Theorem (RTT) can be applied to all the basics laws and re-write them in control volume form. The basic mechanical laws considered for the RTT will now be presented(7).

$$m_{syst} = const, \vee, \frac{dm}{dt} = 0 \tag{A.1}$$

Equation A.1 above is conservation of mass, it is fixed and do not change. m_{syst} is the mass for a system and is constant(7).

$$\mathbf{F} = m\mathbf{a} = m\frac{d\mathbf{V}}{dt} = \frac{d}{dt}\Big(m\mathbf{a}\Big) \tag{A.2}$$

Equation A.2 above is Newton´s second law of motion. If a system have unbalanced forces, leaving a residual force acting on the mass and expose it for acceleration. **F** is the net force, **a** is the acceleration and **V** is the velocity of the mass. It is referred to as the linear momentum relation within fluid dynamics(7).

$$\mathbf{M} = \frac{d\mathbf{H}}{dt} \tag{A.3}$$

The third relation presented, equation A.3 above is the angular momentum exerted if a net moment $\mathbf{M}$ is present. It is a rotational effect and $\mathbf{H} = \sum \Big(\mathbf{r} \times \mathbf{V}\Big)\delta m$ is the angular momentum around the centre of mass. Just as Newton´s 2nd law, this is a vector relation and stretches in the x-,y- and z-direction(7).

$$\delta Q \text{ - } \delta W = dE, \vee, \dot{Q} \text{ - } \dot{W} = \frac{dE}{dt} \tag{A.4}$$

Equation A.4 is the first law of thermodynamics. δQ is added heat to the system, δW is work performed on the surroundings by the system and dE is the system energy and must change according to the relation prescribed(7).

A.1.1 Reynolds Transport Theorem

The universal mechanical laws for system analysis can be converted to fluid dynamics by observing specific regions rather than masses. To enable this, RTT is used and can be adopted using equations A.1-A.4. The specific region observed is enclosed by a control volume (CV) for enabling study of the flow for instants in time. Applying a control volume can be seen below(7).

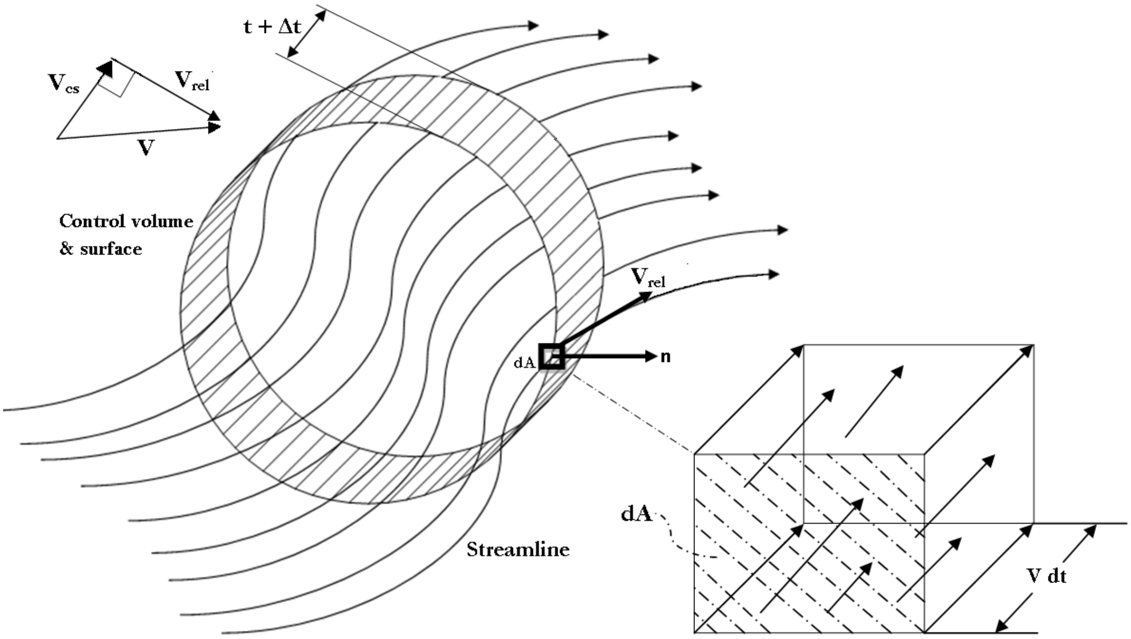

Figure A.1: Control volume enclosing a fluid flow.

The control volume can be stationary, in movement or deformable depending on the circumstances. The velocity relation $\left(\mathbf{V}_{rel} = \mathbf{V} - \mathbf{V}_{cs}\right)$ shows the relative movement. Where $\mathbf{V}$ is the fluid velocity and $\mathbf{V}_{cs}$ is the control surface velocity. If the control volume is stationary we have $\mathbf{V}_{cs} = 0$ and no relative velocity is present, fluid or flow velocity is equal to the control volume´s. dA is an infinite small surface element on the control surface. For every other element dA, the velocity can vary. Therefore, to obtain the total flow properties all elements dA needs to be integrated over the whole surface. What gives the control volume depend on the flow speed $\left(\mathbf{V}\right)$ and how long the time instant (dt) for observation is. Thus, dV = dA $\cdot$ $\mathbf{V}$dt is one volume element and while integrated, the whole volume is obtained for the observed flow. If integration of an arbitrary flow with an arbitrary control volume is adopted, the general RTT can be stated as followed(7):

$$\frac{d}{dt}\left(B_{syst}\right) = \frac{d}{dt}\left(\int_{cv} \beta\rho dV\right) + \int_{cs} \beta\rho\left(\mathbf{V_{rel}} \cdot \mathbf{n}\right)\mathrm{dA} \tag{A.5}$$

$$\frac{d}{dt}\Big(\int_{cv}\beta\rho dV\Big) = \int_{cv}\frac{\partial}{\partial t}\beta\rho dV \tag{A.6}$$

$$\mathbf{V_{rel}}\cdot\mathbf{n} = \mathbf{V_{rel}}\cos\theta = V_n \tag{A.7}$$

$$\int_{cs}\beta\rho\Big(\mathbf{V_{rel}}\cdot\mathbf{n}\Big)\mathrm{dA} = \int_{cs}\beta\rho V_n dA_{out} \text{ - } \int_{cs}\beta\rho V_n dA_{in} \tag{A.8}$$

$$B_{syst} = \Big[m, m\mathbf{V}, \mathbf{H}, E\Big],\ \beta = \frac{dB_{syst}}{dm} \tag{A.9}$$

In equation A.5 and A.9 above, the left hand side concern the system property exposed for analysis where the mechanical system $\Big(B_{syst}\Big)$ can be either mass $\Big(\mathrm{m}\Big)$, momentum $\Big(m\mathbf{V}\Big)$, momentum torque $\Big(\mathbf{H}\Big)$ or energi $\Big(\mathrm{E}\Big)$. B_{syst} can be any vector or scalar property of the fluid. By letting B_{syst} represent one of the mechanical properties presented in equation A.9 the RTT can be re-written from its general form in equation A.5 with the control volume approach. In the general RTT equation $\Big(\mathrm{A.5}\Big)$, the right hand side will be further explained before derivation of RTT special cases. The first term, $\frac{d}{dt}\Big(\int_{cv}\beta\rho dV\Big)$, is the change within the control volume (CV) with ρ as the density and β as the amount of B_{syst} per unit mass. Note that CV and CS stand for "control volume" and "control surface" respectively. The second term describes the flow in and out over the control surface and is often referred to as the flux term. Considering the flux term, the sign convention depends on the direction of the normal unit vector ($\mathbf{n}$) and V_n is the cosine or normal component of the relative velocity. Continuously, special cases of the RTT will be presented, i.e. the continuity (mass conservation), momentum and energy equation(7).

A.1.2 Mass conservation

Equations A.1 and A.5 - A.9 are used in the general RTT, but now narrowed down for the special case of mass conservation. Thus, making the conversion from the mechanical system law A.1 with the RTT adoption(7):

$$B_{syst} = m,\ \beta = \frac{dB_{syst}}{dm} = \frac{dm}{dm} = 1 \tag{A.10}$$

$$\left(\frac{dm}{dt}\right)_{syst} = 0 = \frac{d}{dt}\Big(\int_{cv}\rho dV\Big) + \int_{cs}\rho\Big(\mathbf{V_{rel}}\cdot\mathbf{n}\Big)\mathrm{dA} \tag{A.11}$$

Equation A.13 above is under the assumption of constant mass. With additional assumptions it can be re-written further(7):

$$\mathbf{V_{cs}} = 0\ \Rightarrow \mathbf{V_{rel}} = \mathbf{V} \tag{A.12}$$

The expression above consider a fixed stationary control volume rather than a deformable one. The expression develops to the following state being(7):

$$\int_{cv}\frac{\partial\rho}{\partial t}dV + \int_{cs}\rho\Big(\mathbf{V}\cdot\mathbf{n}\Big)\mathrm{dA} = 0 \tag{A.13}$$

Assuming one-dimensional flow with "n" and "m" number of inlets and outlets respectively, the expression can be developed as stated below(7):

$$\int_{cv} \frac{\partial \rho}{\partial t} dV + \sum_{m} \Big(\rho_m A_m \mathbf{V_m}\Big)_{out} - \sum_{n} \Big(\rho_n A_n \mathbf{V_n}\Big)_{in} = 0 \tag{A.14}$$

The expression above is for one-dimensional compressible flow, i.e. unsteady flow within the control volume. If steady flow is considered, the following equation can be motivated(7):

$$\frac{\partial}{\partial t} = 0 \Rightarrow \int_{cv} \frac{\partial \rho}{\partial t} dV = 0 \tag{A.15}$$

It is important to remark that a flow can be unsteady and in-compressible, but will still lead to the same conclusion as above. If the fluid flow is in-compressible, the density will be constant and the derivative will anyhow disappear. The implication essentially leads to the elimination of the change within the control volume and only the flux term can be considered from now on(7):

$$\sum_{n} \Big(\rho_n A_n \mathbf{V_n}\Big)_{in} = \sum_{m} \Big(\rho_m A_m \mathbf{V_m}\Big)_{out} \Leftrightarrow \sum_{n} \Big(\dot{\mathbf{m}}_n\Big)_{in} = \sum_{m} \Big(\dot{\mathbf{m}}_m\Big)_{out} \tag{A.16}$$

Finally, if inlets and outlets are not considered one-dimensional, the upper expression has to be integrated over the cross section instead(7):

$$\dot{\mathbf{m}}_{cs} = \int_{cs} \rho \Big(\mathbf{V} \cdot \mathbf{n}\Big) dA \tag{A.17}$$

A.1.3 The Linear Momentum Equation

In similar fashion as for the conservation of mass, the linear momentum equation will now be derived. The first derivation was very detailed and the other following derivations wont have the same refinement unless something new is to be presented. Applying the assumptions for the momentum equation leads to the following equations and expressions using equations A.2 and A.5 - A.9. Thus, utilizing Newton´s 2nd law with Reynolds transport theorem to successfully make the conversion form a mechanical mass system perspective to the one of a control volume(7):

$$B_{syst} = m\mathbf{V},\ \beta = \frac{dB_{syst}}{dm} = \frac{dm\mathbf{V}}{dm} = \mathbf{V}, \mathbf{V_{cs}} = 0\ \Rightarrow \mathbf{V_{rel}} = \mathbf{V} \tag{A.18}$$

$$\sum \mathbf{F} = \left(\frac{dm\mathbf{V}}{dt}\right)_{syst} = \frac{d}{dt}\Big(\int_{cv} \mathbf{V} \rho dV\Big) + \int_{cs} \mathbf{V} \rho \Big(\mathbf{V} \cdot \mathbf{n}\Big) \mathrm{dA} \tag{A.19}$$

To be noted is the non-existent density (ρ) contribution in the control volume term. Adding one-dimensional inlet and outlet flow, steady flow or the property of an in-compressible fluid as previously explained leaves us with the final expression:

$$\sum \mathbf{F} = \sum_{m} \Big(\dot{\mathbf{m}}_{\mathbf{m}} \mathbf{V_m}\Big)_{out} - \sum_{n} \Big(\dot{\mathbf{m}}_{\mathbf{n}} \mathbf{V_n}\Big)_{in} \tag{A.20}$$

The force $\mathbf{F}$ is hereby a vector $\mathbf{F} = \Big[F_x, F_y, F_z\Big]$.

A.1.4 The Energy Equation

Reynolds transport theorem is applied on the first law of thermodynamics, using equations A.4 and A.5 - A.9 and the following can be obtained:

$$B_{syst} = E,\ \beta = \frac{dB_{syst}}{dm} = \frac{dE}{dm} = e, \mathbf{V_{cs}} = 0\ \Rightarrow \mathbf{V_{rel}} = \mathbf{V} \tag{A.21}$$

$$\frac{dQ}{dt} \text{ - } \frac{dW}{dt} = \frac{dE}{dt} = \frac{d}{dt}\Big(\int_{cv} e\rho dV\Big) + \int_{cs} e\rho\Big(\mathbf{V}\cdot\mathbf{n}\Big)\mathrm{dA} \tag{A.22}$$

$$e = e_{internal} + e_{kinetic} + e_{potential} = \hat{h} + \frac{1}{2}\mathbf{V}^2 + \mathbf{g}z \tag{A.23}$$

Where positive Q and negative W implies heat added to the system and worked performed by the system, respectively. "e" is the energy per unit mass and consists of multiple contributions regarding internal-, kinetic- and potential energy. After additional work on the expression, which can be further studied in Frank. M. White´s 7th ed. of "Fluid Mechanics" pp.188-190, the final product is:(7)

$$\dot{Q} \text{ - } \dot{W}_s \text{ - } \dot{W}_v = \frac{\partial}{\partial t}\Big[\int_{cv}\Big(\hat{h} + \frac{1}{2}\mathbf{V}^2 + \mathbf{g}z\Big)\rho dV\Big] + \int_{cs}\Big(\hat{h} + \frac{1}{2}\mathbf{V}^2 + \mathbf{g}z\Big)\rho V_n dA \tag{A.24}$$

Where $\dot{W}_s$ is the work performed from an arbitrary machine and $\dot{W}_v$ is the shear work due to viscous stresses of the control surface.

$$\dot{W} = \dot{W}_{shaft} + \dot{W}_{press} + \dot{W}_{visc} = \dot{W}_s + \dot{W}_p + \dot{W}_v \tag{A.25}$$

Where $\dot{W}$ is the net rate work for a stream surface (SS) and $\dot{W}_p$ is pressure forces occurring on the control surface only.

$$\dot{W}_p = \int_{cs} p\Big(\mathbf{V}\cdot\mathbf{n}\Big)dA,\ \dot{W}_v = \text{-}\int_{cs} \tau\cdot\mathbf{V}dA \tag{A.26}$$

Where "τ" is the stress vector on the surface "dA" and is dependent on the specific surface attribute. "p" is the pressure force on a small surface element "dA".

$$\dot{W} = \dot{W}_s + \int_{cs} p\Big(\mathbf{V}\cdot\mathbf{n}\Big)dA \text{ - } \int_{cs}\Big(\tau\cdot\mathbf{V}\Big)_{ss}dA \tag{A.27}$$

$$\hat{h} = \hat{u} + \frac{p}{\rho} \tag{A.28}$$

Equations A.27 and A.23 are substituted into A.22. Adding substitutions of equations A.23 and A.28 give the final expression for the energy equation stated in equation A.24 above. If an one-dimensional assumption is adopted for the final expression, the flux term adjust accordingly to equation A.29 below:(7)

$$\int_{cs}\Big(\hat{h} + \frac{1}{2}\mathbf{V}^2 + \mathbf{g}z\Big)\rho V_n dA = \sum\Big(\hat{h} + \frac{1}{2}\mathbf{V}^2 + \mathbf{g}z\Big)_{out}\dot{\mathbf{m}}_{out} \text{ - } \sum\Big(\hat{h} + \frac{1}{2}\mathbf{V}^2 + \mathbf{g}z\Big)_{in}\dot{\mathbf{m}}_{in} \tag{A.29}$$

A.2 Emission Result

This section present the remaining results not discussed, emission predictions. Firstly, the carbon oxides are presented and sequentially the hydrocarbons and the carbon-dioxides. For every other species (except CO_2) there will be three plots each for deeper understanding. All plots presented outweigh simulation data against measurements. First off, an error percentage plot will appear. Secondly comes, a plot showing the ppm (parts per million) difference in absolute values. Lastly, a plot of ppm absolute values will be presented to show if the trend is on the path.

A.2.1 NO_x, Nitrogen Oxides

From hereon the NO_x species will be reviewed according to the structure stated above.

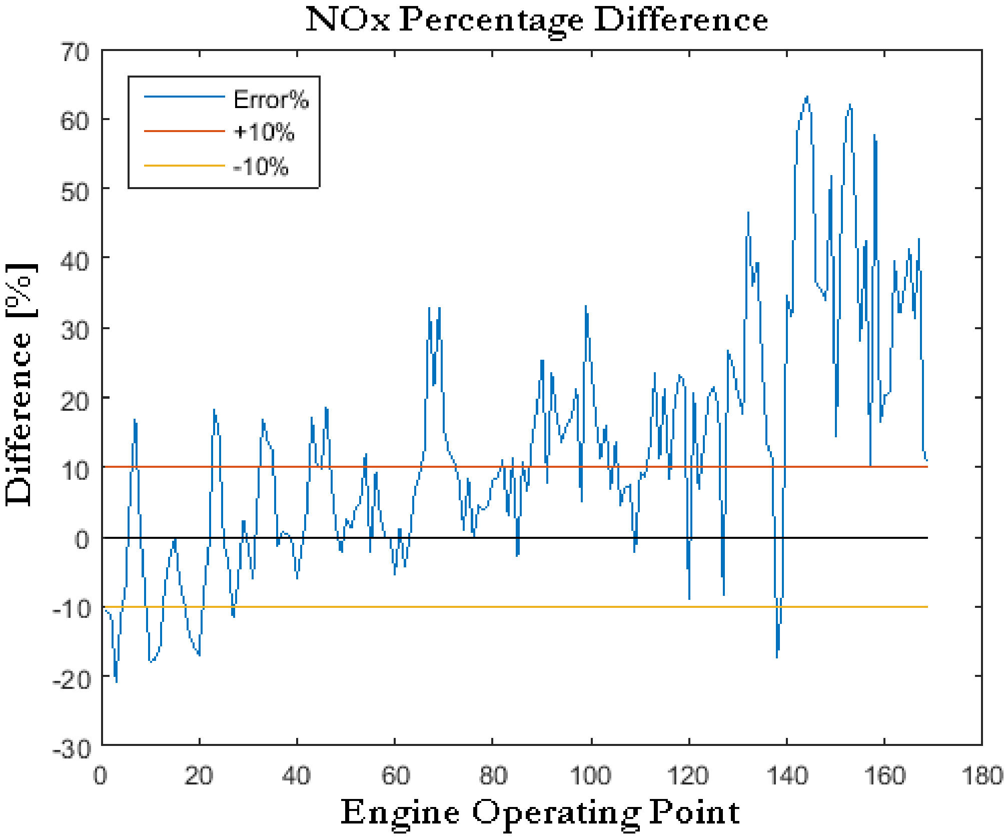

Figure A.2: NO_x percentage difference, simulated versus measurements.

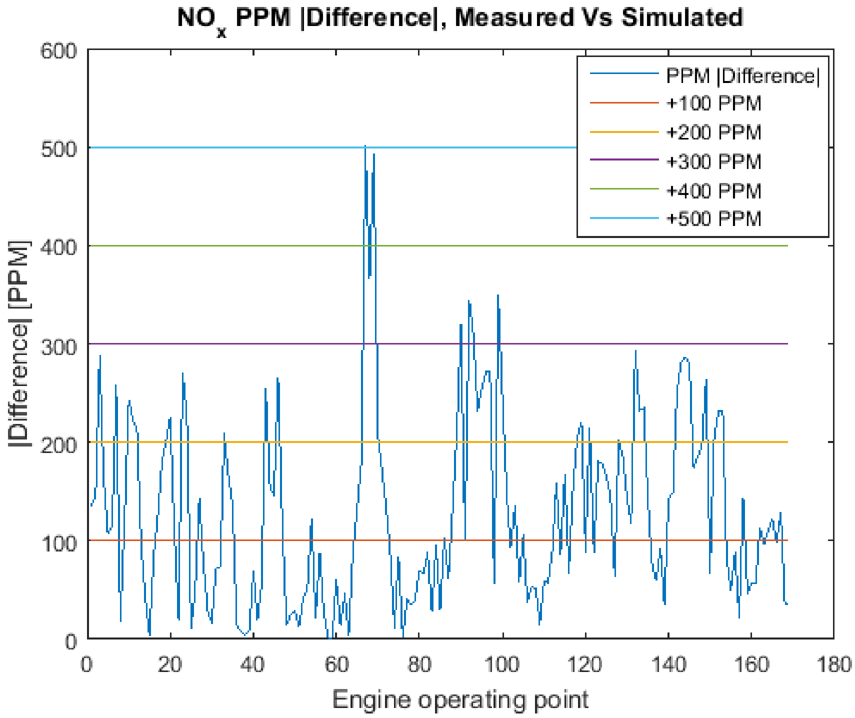

Figure A.3: NO_x ppm absolute difference, simulated versus measurements.

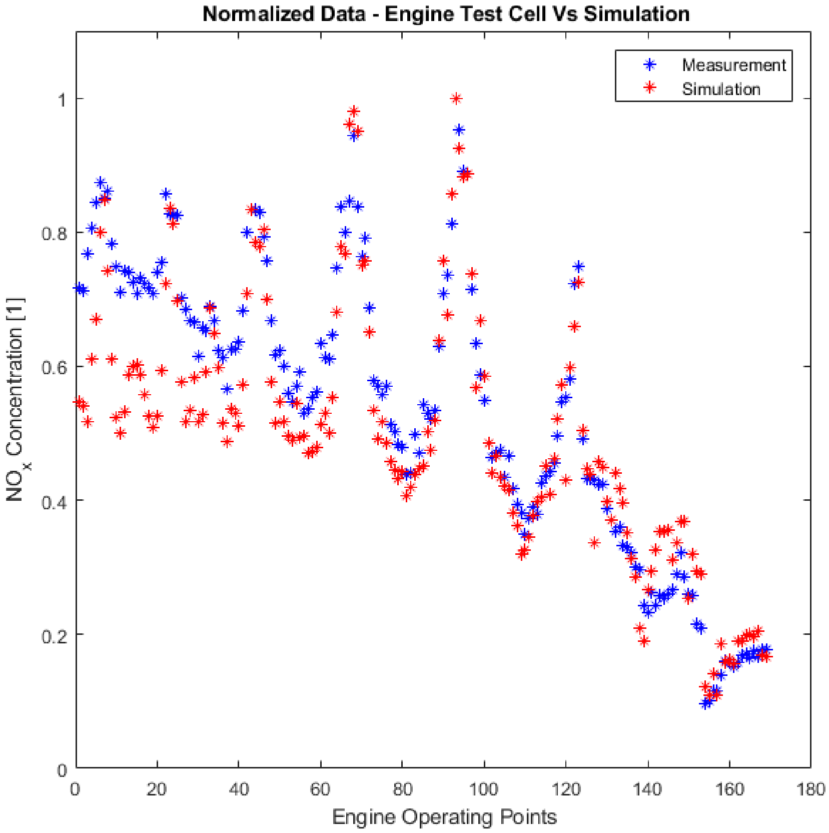

Figure A.4: Normalized NO_x ppm values, simulated versus measurements.

In the most upper plot, figure A.2, the NO_x error percentage can be seen. The tolerance had a limit of 10%. Further plots are presented to show a broader analysis on why the graph looks as such, referring in sequential order figure A.3 and A.7. The latter figures mentioned show that the majority of the points have a deviation of about 100 ppm in absolute difference comparison. And if the very last plot (A.7) with the absolute values are overseen, it does not look that bad as the very first percentage plot would suggest. That motivates why all these plots were used for this one species. The presentation of the data can be miss-leading if not fully investigated. The last plot are for example normalized with the data set´s maximum value.

A.2.2 HC, Hydrocarbons

From hereon the HC species will be reviewed according to the structure stated above and in the same spirit as of the carbon oxides.

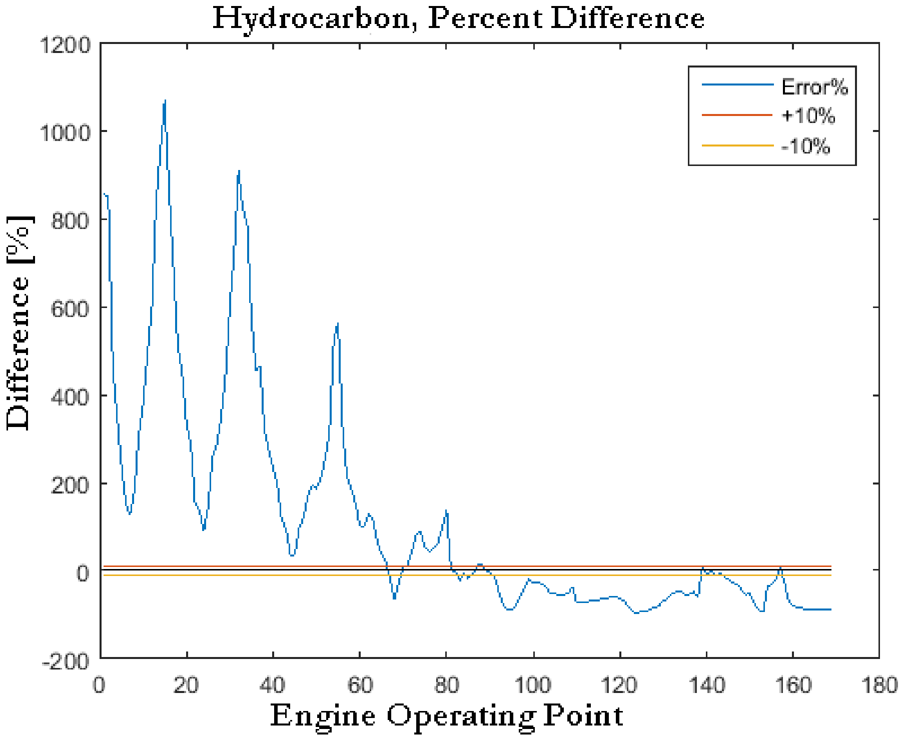

Figure A.5: HC error percentage, simulated versus measurements.

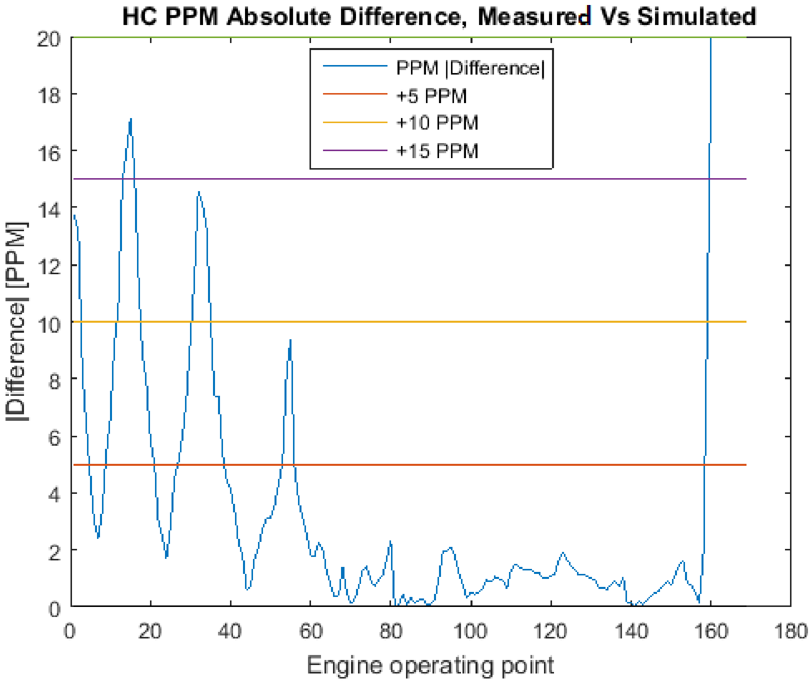

Figure A.6: HC ppm absolute difference, simulated versus measurements.

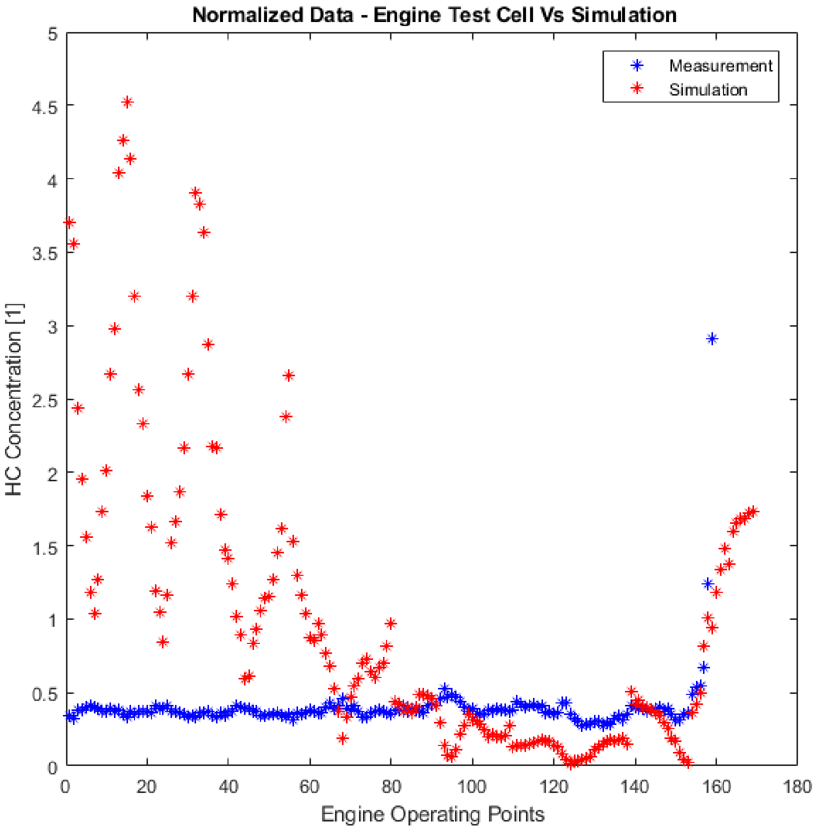

Figure A.7: Normalized HC ppm data, simulated versus measurements.

In the most upper plot, figure A.5, the HC error percentage can be seen. The tolerance had a limit of 10%. Further plots are presented to show a broader analysis on why the graph looks as such, referring in sequential order figure A.6 and A.7. The latter figures mentioned show that the majority of the points have a deviation of about 1 or 2 ppm in absolute difference comparison. And if the very last plot (A.7) with the absolute values are overseen, it can be seen why this was a particular tricky species to capture. The graph is normalized due to the project´s confidentiality. The measured values are to begin with really low for the majority of the engine points. It is just until the low load points, talking about injected masses in the quantity of a few unit singular milligrams. The significant HC quantities, counting ten of ppms, starts at the 160th engine operating point of the 169 available and could perhaps therefore be overlooked.

A.2.3 CO_2, Carbon-dioxides

From hereon the CO_2 species will be reviewed as followed down below.

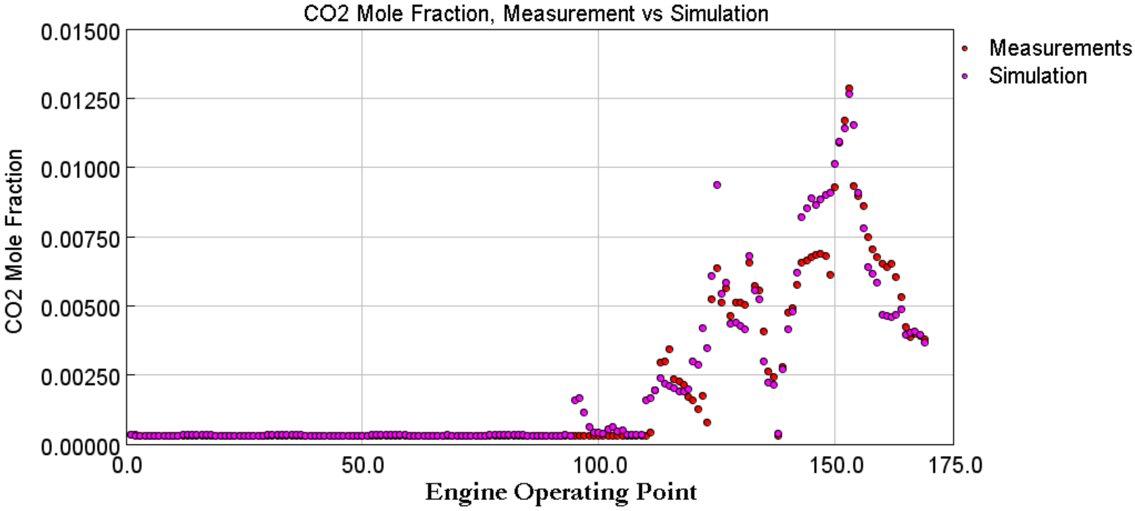

Figure A.8: CO_2 mole fraction absolute values, simulated versus measurements.

In figure A.8 the CO_2 mole (volume) fraction can be perceived. The mole fraction property is a way to target the correct amount of EGR-% and can be read more about in appendix section A.3.13. By reviewing the figure, it can be stated that the targeting is of a decent nature, but could be improved.

A.3 FRM General Modelling Blue Print

In section A.3 the connections, measurement inputs, simulation inputs, calibration parameters, design constants and default values are pointed out and explained thoroughly. Starting with the intake components on the cold side and continue downstream all the way through the cylinders to the hot side´s exhaust pipes. The figures are from the point in time were the FRM was fully calibrated and final in such. However, it looked slightly different when the Simulink Harness integration was implemented. The implementation required to replace all controllers with maps instead. Thus, the mapping procedure is also covered for the components concerned. "Measurement inputs" are measured data from an engine test cell. "Simulation data" is either extracted values from a simulation or values to impose component limits. "Calibration parameters" are parameters which have been optimized using GT´s optimizer tool. "Design constants" are all physical data giving the engine its geometry or performance. "Default constants" have the same quantity and values suggested initially by GT-POWER. Initial conditions such as temperature, pressure and humidity is not presented as they occur for every volume. "Discretization length" will not be addressed as it as already heavily covered in chapter 2.2. If one of these sub-headings is missing, it means there was nothing to include or it has already been mentioned.

A.3.1 Intake Environment

Connection:
This object connects to the intake pipes. The component can be seen in figure A.9.

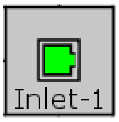

Figure A.9: Intake Environment

Description:
This object describes ambient conditions such as temperature, pressure, humidity and fluid composition.

Measurement inputs:
Pressure, temperature and humidity.

Default constants:
Fluid properties.

A.3.2 Intake Pipes

Connection:
This object connects the ambient environment and the compressor. It includes a pipe and a restriction object (bellmouth). The component can be seen in figure A.10.

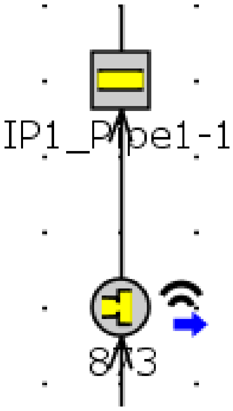

Figure A.10: Intake Pipes

Description:
The typical representation of the simplified piping system. In every volume a computation is done, how often depends on the discretization length. How the computation is performed depends on which solver is used, explicit or implicit see theory chapter 2.2.1. The restriction uses a diameter to limit the flow, the pipe model correct surface area and volume for the intake pipes and is also needed for the compressor later on. The restriction´s orifice diameter is used for calibration and is varied to achieve correct compressor

inlet pressures. The same analogy can be applied to Friction Multiplier (FM) and Heat Transfer Multiplier (HTM). Greater diameter implies more air particles and hence more particle and wall collisions establishing the pressure required. The FM accounts for pressure drop losses, the greater FM, more wall friction and hence greater pressure drops. Greater HTM means more heat transfer will occur and dissipate according to convection. The bellmouth will have an overhead diameter if used between the exhaust manifolds.

Calibration parameters:
FM, HTM, orifice diameter.

Design constants:
Pipe length, inlet diameter or bore (equation relating bore and inlet diameter), overhead diameter.

Default constants:
Fluid properties, discretization length, number of holes and hole thickness. Last two if used between two exhaust manifolds.

A.3.3 Compressor

Connection:
This object connects the intake pipes, turbocharger shaft and boost pipes (CAC). The component can be seen in figure A.11.

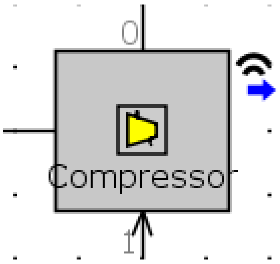

Figure A.11: Compressor object

Description:
Represents a compressor in a supercharged or turbocharged engine. It is of great importance of neighboring volumes to have correct diameters because this object use velocities and calculates the total pressure ratio taken from the nearby sub-volumes. Different compressors are available depending on the user´s available data, with more data the further detailed and trust-able predictions. GT-SUITE predicts turbine or compressor speed and Pressure-Ratio (PR) at each timestep and are therefore known (because of the map look-ups). The massflow rate and efficiency are later on looked up and imposed in the solution. Compressors are very sensitive though, the massflow rate can fluctuate rapidly sometimes. It happens because of the stall ("surge") line is crossed just a bit or when the speed lines are very flat, thus small changes in PR results in large massflow changes. Upon that, the code has a damping mechanism with a real physical meaning, it´s the natural damping of the air mass and momentum in the compressor. This reduces the compressor´s extreme massflow rate fluctuation magnitudes. The massflow rate is later on imposed in the adjacent volume borders, and may be damped as stated. The outlet temperatures is calculated using enthalpy changes across the turbine and the compressor. The change in enthalpy, and hence the power created or used is calculated from their specific efficiency equations(5).

Calibration parameters:
PR, massflow and efficiency. If the map is not matching the compressor performance, it can be optimized by varying these parameters.

Design constants:
Rack position, compressor map.

A.3.4 Charge Air Cooler (CAC)

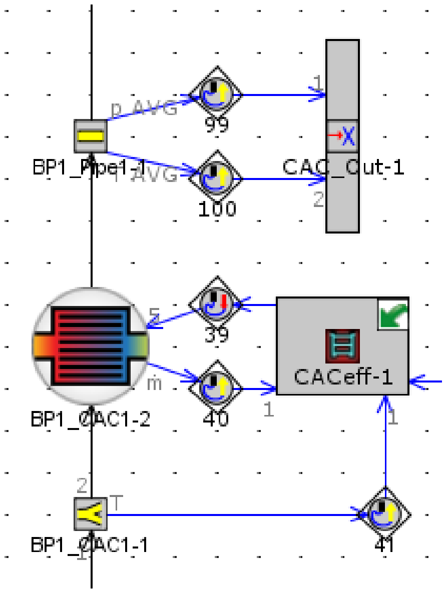

Figure A.12: CAC object

Connection:
This object connects the compressor and CAC-throttle. To describe the CAC technology there are three objects used; The pipe object as previously presented, the heat ex-changer object and the flow split volume. The components can be seen in figure A.12.

Description:
The heat exchange object is typically used for FRMs (Fast Running Models) used in RT (Real-Time) applications. The flow split is an alternative piping, when multiple openings exists (5). A performance approach can be used instead, but usually causes solver instability due to large time steps. The meaning of this heat ex-changer is to deliver an outlet CAC temperature and can be more or less predictive. Here the a semi-predictive efficiency approach is used. The intercooler outlet temperature is still imposed, but is calculated through the efficiency, CAC inlet and coolant temperature. The efficiency is looked-up using massflow rate, whereas higher massflow result in decreasing CAC efficiency(4). This component highly determines the airflow and is another sub-system up for calibration. It should be calibrated early as the other components in the engine aligns after the airflow calibration. The orifice diameter is varied in the heat ex-change object to meet compressor outlet pressures.

Measurement inputs:
RPM, injected mass, CAC outlet temperature and ambient temperatures.

Calibration parameters:
The orifice diameter, HTM and FM.

Design constants:
Volume (bore related equation), surface area, length, expansion diameter (bore related equation).

Default constants:
Discretization length.

A.3.5 CAC-throttle

Connection:
This object connects the CAC, EGR-circuit and the intake manifold. The component can be seen in figure A.13.

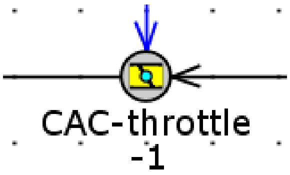
CAC-throttle
-1

Figure A.13: CAC-throttle

Description:
Used to avoid back-pressure, creating a vacuum and let the EGR flow pass in to the intake manifold. Is angled parallel with the flow (90 degrees, fully open) when no EGR is used. Valves, orifices and throttles all requires discharge coefficients (CDs). The CDs are simply a ratio of flow areas, the effective flow area through the reference area to be specific. The CDs originates from the isentropic flow equations through a nozzle. Friction losses and errors in assumed velocity profiles are included, i.e. accounted for. Mathematically, it´s just a ratio over flow rates for the nozzle – actual flow rate over the ideal one (max)(5). The CDs are ideally taken from the specific engine setup, established from laboratory measurements but can also be simulated values.

Measurement inputs:
CDs, CAC-throttle angle.

Design constants:
Reference diameter.

A.3.6 Intake Manifold

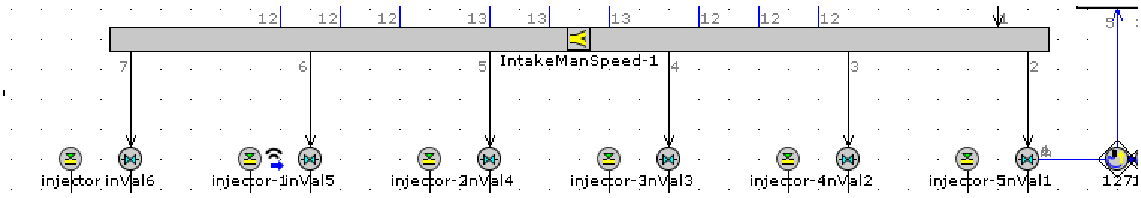
12
12
12
13
13
13
12
12
12
1
5
IntakeManSpeed-1
7
6
5
4
3
2
injector
inVal6
injector-1
inVal5
injector-2
inVal4
injector-3
inVal3
injector-4
inVal2
injector-5
inVal1
1271

Figure A.14: Intake manifold

Connection:
This object connects the EGR-circuit, CAC-throttle and intake valves. It is modelled with another flow split volume. The component can be seen in figure A.14.

Description:
As previously described. However, depending on what kind of component that is

modelled, different material properties can be used and even calibrated. For example, the external convection coefficient has been modified to fit the circumstances of this component using the optimizer. The HTM is calibrated to target compressor outlet pressures.

Calibration parameters:
The external convection coefficient, diameter, HTM and FM.

Design constants:
Boundary conditions such as diameter and characteristic length (bore related), volume (bore related), surface area.

A.3.7 Intake Valves

Connection:
This object connects the intake manifold and the engine cylinder. The component can be seen in figure A.15.

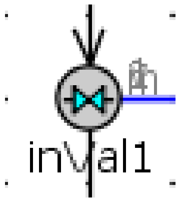

Figure A.15: Valve object

Description:
Describes a cam-driven valve with lift-profile, geometry and flow characteristics. Uses a map for lash clearance height, versus valve face temperature, to define how much it can expand. Lift arrays are used with Crank Angle Degrees (CAD) versus lift[mm]. Further on, the component also utilizes CDs as described earlier with the exception of lift/diameter as X-array. The flow area multiplier can be used in optimization which regulate the effective flow area.

Measurement inputs:
CDs.

Calibration parameters:
Flow area multiplier.

Design constants:
Valve lash clearance, lift profiles (CAD vs lift files), valve reference diameter.

A.3.8 Injectors

Connection:
This object connects to the engine cylinder. The component can be seen in figure A.16.

Figure A.16: Injector object

Description:
This object allows multiple injection pulses, typically used for DI diesel engines. Can use modeling of nozzles to simulate the multiple injection if data is missing. Preferably using injector references and maps from manufacturer to look

up energizing time and unit injector pressure. Mapping which sort out which engine point is

Measurement inputs:
Rail pressure, pre-/main-/post-injected mass, pre-/main-/post-SOI (injection timing), injector rate map (milliseconds (X)/Rail pressure (Y)/ Injection rate (Z)), RPM (X)/Injected mass (Y)/index (Z)-map.

Design constants:
Nozzle hole diameter, number of holes per nozzle, nozzle CD.

Default constants:
Diesel fluid properties.

A.3.9 Cylinder

Connection:
This object connects the injector, intake and exhaust valve. The component can be seen in figure A.17.

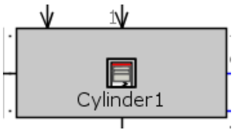

Figure A.17: Cylinder object

Description:
Defines combustion and heat transfer. Can make use of imposed values all the way to fully predictive combustion. The fully predictive combustion is the more desirable since it will adapt to different conditions, which imposed burn rates will not typically do. The cylinder uses temperatures for heat transfer calculation and can be either set or calculated every CA. The cylinder is further divided into zones, to accomplish the heat transfer estimation. There are three cylinder wall zones, three piston zones, three cylinder-head zones and valve face and back areas. If 'WoschniGT' is used, it calculates in-cylinder heat transfer coefficients with the calssical Woschni correlation without swirl(6). DI-pulse will be explained down below in section A.3.9.1. DI-pulse is the fully predictive combustion model for diesel engines.

Simulation data input:
in-cylinder temperatures valve face and back, cylinder zone 1/2/3, piston zone 1/2/3, head zone 1/2/3, burn rate (with SOI and fuel fraction burned), Heat Transfer Model (WoschniGT), convection temperature evaluation.

Calibration parameters:
Valve back heat transfer multiplier.

Design constants:
Head/bore area ratio, piston/bore area ratio.

A.3.9.1 DI-Pulse

DI-pulse is a fully predictive combustion model for diesel engines. The meaning of "predictive" in this context is that the combustion rate is always calculated and not a constant. To manage this, the combustion model attempts to model the most important combustion physics occurring. The model adjust to varying conditions, for example different injected mass, RPM and EGR. Therefore, the benefits are quite evident. Generally, the normal thing to say is that the gain is accuracy and the lost is in simulation run speed. However, the penalty of this implementation or any other use of controllers should not be the cause of a significant drop in simulation run speed(4).

A.3.9.1.1 Cylinder Pressure Matching

The typical combustion calculation use burn rate and calculates cylinder pressure, hence referred to as a "forward" run. With a predictive combustion model, the burn rate is unknown. Therefore a "reverse" run is implemented, using measured cylinder pressure traces to define the burn rates. Cylinder pressure is the input and the burn rate is the output calculated by GT-POWER. The reversed and the forward run use the same two-zone combustion methodology. It implies both methods include the full chemistry and thermodynamics without any simplifications. In the reverse run, fuel transferred from the unburned to the burned zone is iterated within each timestep until the simulated cylinder pressure matches the measured one. The following energy equations are used for the two-zone model and are solved for each timestep(4):

Unburned Zone:

$$\frac{\mathrm{d}(m_u e_u)}{\mathrm{d}t} = \text{-p}\frac{\mathrm{d}V_u}{\mathrm{d}t} \text{ - } Q_u + \left(\frac{\mathrm{d}m_f}{\mathrm{d}t}h_f + \frac{\mathrm{d}m_a}{\mathrm{d}t}h_a\right) + \frac{\mathrm{d}m_{f,i}}{\mathrm{d}t}h_{f,i} \tag{A.30}$$

Where,

m$_u$ = unburned zone mass
e$_u$ = unburned zone energy
p = cylinder pressure
V$_u$ = unburned zone volume
Q$_u$ = unburned zone heat transfer rate
m$_f$ = fuel mass
h$_f$ = fuel mass enthaply
m$_a$ = air mass
h$_a$ = air mass enthalpy
m$_{f,i}$ = injected fuel mass
h$_{f,i}$ = injected fuel mass enthalpy

Burned Zone:

$$\frac{\mathrm{d}(m_b e_b)}{\mathrm{d}t} = \text{-p}\frac{\mathrm{d}V_b}{\mathrm{d}t} \text{ - } Q_b \text{ - } \left(\frac{\mathrm{d}m_f}{\mathrm{d}t}h_f + \frac{\mathrm{d}m_a}{\mathrm{d}t}h_a\right) \tag{A.31}$$

Where index "b" denotes the burned zone and is otherwise similar to equation A.30, but applied for the other zone. In equation A.30 on the right hand side, the first term to the last stands for pressure work, heat transfer, combustion and enthalpy from injected fuel. At each timestep a mixture of fuel and air is translated from the unburned to the burned zone. The starting point of the trapped mass is in the unburned zone, including EGR and residual gases. Later on, the mixture starts to transfer to the burned zone, were the transfer rate is determined of the burn rate and is calculated of the combustion model. Once everything have transferred to the burned zone, a chemical equilibrium is carried out for the whole burned zone. The chemical equation establish the species concentration and when the composition is determined the internal energy can be determined for each species. Further on, all species' internal energies are summed up and the entire burned zone energy is obtained and applying energy conservation gives the zone temperatures and the cylinder pressure(4).

Finally, the simulated pressure has to match the measured one. This usually done by a separate calculation off-set from the project, using the same input measurements and geometry. First off, a coarse burn rate calculation is done using Woschni correlation and assumptions. Secondly, the calculated burn rate is applied during a forward simulation and the heat transfer is saved. Thridly, one final computation of the burn rate is done with the true heat transfer. Lastly, final burn rate is used to provide results for comparing simulation and measurement(4).

A.3.9.1.2 Calibration

Although DI-pulse is fully predictive, it is still derived from simplifications and assumptions. To compensate for this, calibration of a hand full of physical multiplier constants is required. The achievement with these multipliers is to represent the combustion system in the best, and widest operating range possible. The multipliers concerned are namely; entrainment rate, ignition delay, premixed combustion rate, diffusion combustion rate, NO_x calibration and N_2 oxidation activation energy. The mentioned multipliers will tune the injection (spray) and combustion accordingly(4).

Entrainment Rate Multiplier The fuel spray is injected and slows down as the surrounding burned and unburned gases are entrained to the pulse. The mixing of pulses happens through entrainment. The entrainment rate is determined by applying the momentum conservation equation. An empirical relation for spray tip penetration determine the velocity and position. In the end, it affects injector nozzle velocity, breakup time and spray tip length(4).

Ignition Delay Multiplier Based on each pulse and the conditions within it, the ignition delay is computed separately using Arrhenius expression. This factor in- or decrease it(4).

Premixed Combustion Rate Multiplier It is a specific combustion. The present mixture during ignition is set aside for premixed combustion. It has a kinetic rate limitation and this factor in- or decrease it(4).

Diffusion Combustion Rate Multiplier After ignition, the remaining entrained gas and unmixed fuel will mix and combust in a primary diffusion phase. The rate of this sate or phase of combustion can be tuned(4).

NO_x **Calibration Multiplier** Used for prediction of net rate of NO_x formation(4).

N_2 Oxidation Activation Energy Multiplier Multiplies the activation energy of N_2 oxidation rate. Values lower than 1 will increase the NO formation. The inverse will happen for values greater than 1(4).

A.3.10 Exhaust Valves

Connection:
This object connects the cylinder and the exhaust manifold. The component can be seen in figure A.18.

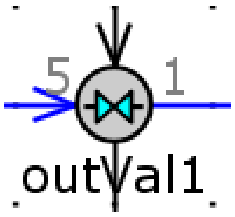

Figure A.18: Exhaust valve

Description:
Uses same parameters and inputs as the intake valve, but for the hot side. However, the exhaust lift has a more thorough lookup. It has a minimum, main and boost lift profile depending on the load. It also simulates a valve leakage. The forward and reverse CDs are for once not the same quantity and the reverse CD has more points (more carefully mapped) since it spans over a greater data range of CDs. The mapping is further different in the sense of data arrays, with static pressure-ratio (X), Lift over diameter (Y) and the CDs as (Z) output.

Measurement inputs:
CDs, static pressure ratio.

Calibration parameters:
The exhaust valve lash could be optimized.

Design constants:
Valve reference diameter (bore equation), lift, exhaust lift profiles, exhaust valve lash.

A.3.11 Crankshaft with auxiliary

Connection:
This object connects to the cylinders and the auxiliary torque. The components can be seen in figure A.19.

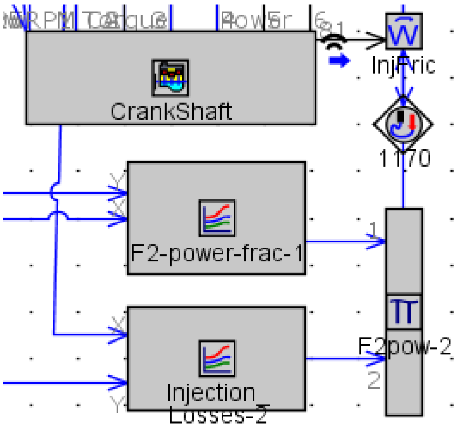

Figure A.19: Crankshaft and auxiliary

Description:
Defines the reciprocating dynamics of the ICE. Translates pressures acting on the pistons to torque acting on the crankshaft. Defines cylinder and crankshaft characteristics such as geometry, cylinder firing and shaft performance. Thus, the engine friction is carefully taken care of. The auxiliary mapping is to model the auxil-

iary losses. The power loss is calculated and transferred via an actuator to a friction object, applied for a rotating part (the crankshaft). It uses two look-ups where a power fraction and an injection power loss is the outcome respectively. The first one uses injected mass and rail pressure to find the power-fraction. The second one uses RPM and injected mass to find the injector´s power consumption.

Measurement inputs:
RPM, mean piston speed, rail pressure.

Simulation inputs:
Injector power fraction and power consumption.

Calibration parameters:
FMEP, peak cylinder pressure factor, mean piston speed squared factor.

Design constants:
Bore, stroke, TDC (Top Dead Center) clearance height, compression ratio, connecting rod length (stroke equation) and CA at IVC (intake valve closing).

A.3.12 Exhaust Manifold

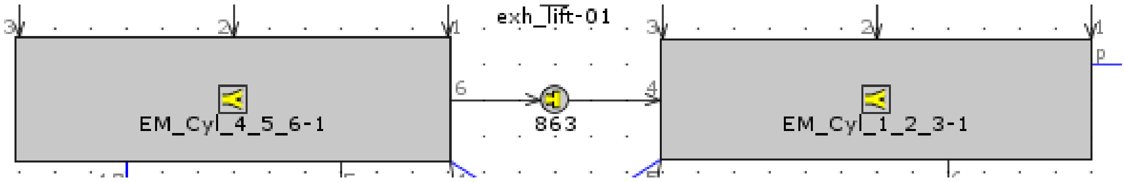

Figure A.20: Exhaust manifold

Connection:
This object connects to the exhaust valves, wastegate and the turbine inlet. The component can be seen in figure A.20.

Description:
It is a flow-split object which has been described previously, the differences will be covered though. It uses imposed exhaust port wall temperatures. The component is utilized for calibration whereas the HTM is varied to achieve measured turbine inlet temperatures, exhaust gases. It has a overhead diameter between both exhaust manifolds.

Measurement inputs:
RPM.

Simulation inputs:
Extracted exhaust port wall temperatures.

Calibration parameters:
HTM and FM.

Design constants:
Expansion diameter (Bore related equation), surface area, volume (Bore related equation).

A.3.13 EGR Pipes

Connection:
This object connects to the exhaust manifold and the volume downstream of the CAC-throttle. The component can be seen in figure A.21.

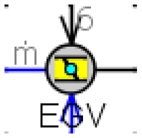

Figure A.21: EGR valve

Description:
It is a direct EGR circuit, meaning it is directed precisely after the exhaust manifold and before the turbine. The pressure depends on what comes out of the cylinder, it is not extra pressurized neither cooled. This is the meaning of the CAC-throttle, to create a "vacuum" environment which naturally will drive the EGR into the intake manifold. The EGR opening can be done in several ways, for example either with a valve or throttle mechanism. In the end, the important data is the CDs, as for any transitioning geometry. The CDs can be laboratory measurements or extracted simulation data. The diameter can and should be calibrated against either EGR percentage or CO2 mole (volume) fraction. The PID-controller is used to target the CO2 fraction. The controller is replaced with mapping when the RT-version comes to place. The map-values need to be optimized every time a significant change is performed in the engine. The engine management system (EMS) signal which goes from zero to hundred percent needs to be correlated to the throttle angle. Therefore, the throttle angle is optimized once again against the CO2 mole fraction and later plotted against the EMS-signal. From there, a trend-line can be tracked to fit the data in the most appropriate manner possible. Manual intervention can occur. Lastly, the values are created in the map and imposed. The same procedure is done for the CAC-throttle.

Simulation inputs:
CDs, reference diameter (overridden).

Calibration parameters:
The orifice diameter or/and the EGR-valve map.

A.3.14 Turbine

Connection:
This object connects to the exhaust manifold, turbocharger shaft and the exhaust pipes. The component can be seen in figure A.22.

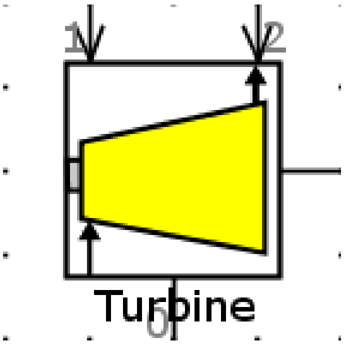

Figure A.22: Turbine object

Description:
It functions as explained in compressor section A.3.3 regarding the mapping. The turbine can be calibrated instead of changing the waste-gate diameters. By varying the turbine massflow and efficiency multipliers to minimize the difference between measured boost pressure and simulated.

Measurement inputs:
Engine RPM. (map includes turbo RPM, massflow, efficiency and PR)

Simulation inputs:
Maximum pressure ratio, maximum speed (reduced).

Calibration parameters:
Massflow and efficiency multipliers, efficiency shape factor at low BSR, efficiency intercept at high BSR, massflow ratio at 0 BSR, massflow ratio exponent.

Design constants:
Rack array and turbine map.
Default constants:
Waste-gate diameter.

A.3.15 Wastegate

Connection:
This object connects to the exhaust manifold, compressor downstream volume and turbine downstream volume. The component can be seen in figure A.23.

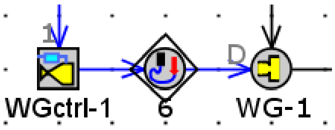

Figure A.23: Wastegate object

Description:
Whenever the boost pressure is too high, the exhaust gases is bypassed the turbine via the WG. The WG diameter proportion depends on what pressure the compressor downstream volume measures. It can be controlled and actuated which is recommended. Any controllers used usually do not slow down the computation significantly. However, in the case of a RT-model, any controls cannot be used and have to be replaced by some sort of mapping.

Measurement inputs:
Compressor outlet pressure.

Design constants:
Maximum turbo speed, maximum WG diameter, initial WG diameter and its duration.

A.3.16 Turbo Shaft

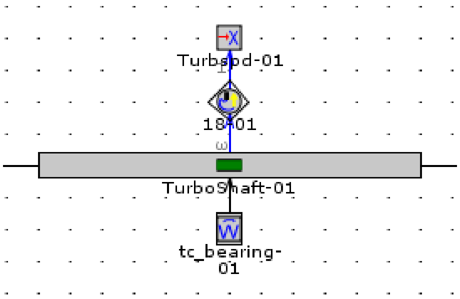

Figure A.24: Turbo shaft object

Connection:
This object connects to the turbine and the compressor. The component can be seen in figure A.24.

Description:
The shaft object is used whenever the inertia of a rotating part is of importance. The model is 1D-rotational. The significance of this object lies in the ‘Mechanical efficiency’ attribute. The attribute is used during simulation in order to model the losses by applying a friction torque between the object and the ground. In this case, the ‘Mechanical Efficiency’ attribute is “def” which imply the efficiency is 100%. Instead the ’tc-bearing-01’ is used, implying the losses directly on to the shaft by adding “negative” energy on to the shaft. Input torque is known, the absolute losses and hence the output torque and power. The torques of compressor and turbine powers are used to calculate turbocharger shaft speed. The result is a speed dependent mapping of the power-loss due to inertia.

Measurement inputs:
Turbine speed.

Simulation inputs:
Shaft power-loss mapping.

Design constants:
Static torque, initial angular position, shaft moment of inertia.

Default constants:
Mechanical efficiency.

A.3.17 Exhaust Pipes

Connection:
This system connects to the turbine, wastegate and the ambient environment. The component can be seen in figure A.25.

Description:
Previously described in section A.3.2. This system of pipes is the last component up for calibration. The exhaust pipe orifice diameter is varied until turbine outlet pressures are achieved.

Calibration parameters:
FM, HTM, orifice diameter.

Design constants:
Pipe length, inlet diameter or bore (equation relating bore and inlet diameter), overhead diameter.

Default constants:
Number of holes and hole thickness. Last two if used between two exhaust manifolds.

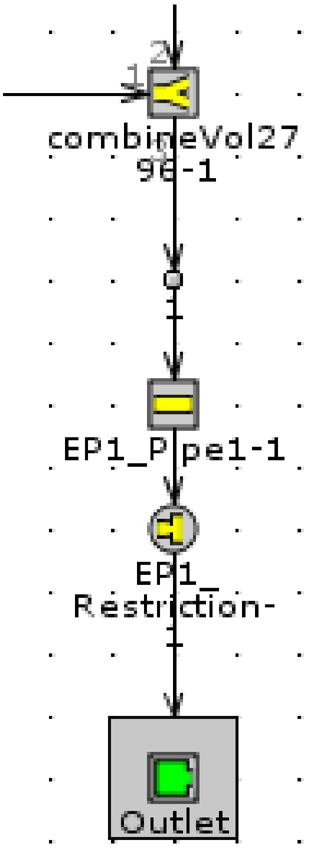

Figure A.25: Exhaust pipes